# User Manual

TOUGH 2-GRS
Version 2
TOUGH 2-MP-GRS
Version 0

**Gesellschaft für Anlagen- und Reaktorsicherheit (GRS) gGmbH**

# User Manual

TOUGH2-GRS
Version 2

TOUGH2-MP-GRS
Version 0

Martin Navarro

September 2018

**Remark:**

# Kurzfassung

Die Codes TOUGH2 und TOUGH2-MP, die vom Lawrence Berkeley National Laboratory, Kalifornien, USA, entwickelt wurden, simulieren mehrphasige Strömungsvorgänge in porösen Medien. Die GRS verwendet TOUGH2-Codes seit 1991 im Rahmen von Prozess- und Langzeitsicherheitsanalysen für tiefe geologische Endlager und hat den Code im Laufe der Jahre um weitere, endlagerrelevante Prozesse erweitert. Im Vorhaben 4715E03230 des BMU wurden diese Entwicklungen fortgeführt und auf den parallelisierten Code TOUGH2-MP portiert. Der vorliegende Bericht beschreibt die resultierenden Codes TOUGH2-GRS und TOUGH2-MP-GRS.

# Abstract

The codes TOUGH2 and TOUGH2-MP, which have been developed by the Lawrence Berkeley National Laboratory, California, USA, simulate multi-phase flow in porous media. GRS uses TOUGH2 codes since 1991 to conduct process analyses and safety assessments for deep geological repositories and it has added new processes to the code that are relevant to repository systems. Within BMU project 4715E03230, new developments have been made and the code extensions have been ported to the parallelized code TOUGH2-MP. The present report describes the resulting codes TOUGH2-GRS and TOUGH2-MP-GRS.

# Table of Contents

# 1        Introduction

TOUGH2 is a code for the simulation of multi-phase flow in porous media and has been developed at the Lawrence Berkeley National Laboratory, California, USA /PRU 99/. TOUGH2-MP /ZHA 08/ is a multi-processor version of TOUGH2. TOUGH2 as well as TOUGH2-MP are used by GRS to simulate multi-phase flow and radionuclide transport in repository systems for radioactive waste.

Since 1992, GRS is supplementing the code TOUGH2 by physical processes that are relevant to repository systems. Early code modifications have focused on repository concepts for rock salt and included porosity and permeability changes due to salt creep /JAV 95/, which is a driving process for barrier sealing in such concepts. Non-linear and brine-dependent sorption was implemented to simulate the transport of radionuclides in the far-field of a repository /JAV 01/, /JAV 02/, /FIS 01/. Later on, the focus shifted to argillaceous host rocks. From 2006 to 2008, a porosity model for immobile water was introduced /NAV 08/ as well as the process of dilating micro fissures, known under the name pathway dilation /NAV 09/. The pathway dilation model was applied in the FORGE project in order to explain gas injection experiments conducted in the Mont Terri underground research laboratory /NAV 13a/. In the course of this project, new mechanisms of pathway dilation including kinetic dilation processes were added.

Until 2009, most of the TOUGH2 modifications conducted by GRS had been realized independently. Integration and improvement of previous modifications was attempted between 2009 and 2012 in BMU project 3609R03210, resulting in the code TOUGH2-GRS version 0 /NAV 13b/. This codes was extensively used in the VSG project, a preliminary safety analysis for the Gorleben site (BMU project UM10A03200, /LAR 13/, /KOC 12/).

The shift to version 1 /NAV 16a/, was undertaken in project ZIESEL (UM13A03400, /KOC 16/). The code version was subject to extensive quality assurance, particularly by means of the automatic code testing programme SITA developed by GRS /SEH 16/, /NAV 18/, /HOT 17/.

In BMU project 4715E03230, anion exclusion and temperature-dependent capillary pressures have been introduced to the code. Further on all code extensions of GRS were ported to the multi-processor code TOUGH2-MP. The resulting code was called

TOUGH2-MP-GRS. Both codes, TOUGH2-GRS and TOUGH2-MP-GRS, are described in this report, which is an update of Navarro & Eckel 2016 /NAV 16a/. Most features of TOUGH2-MP-GRS resemble the features of TOUGH2-GRS, so that most parts of this report apply to both codes. Exceptions from this rule will be mentioned.

# 2        General code features

## 2.1        Code basis

The code TOUGH2-GRS is based on the code TOUGH2, version 2.0, and on the solver package T2SOLV (files t2cg22.f and t2solv.f) of TOUGH2 version 2.1. Bugfixes for TOUGH2 v. 2.0 have been published on the LBNL website /LBNL 16/ and included in TOUGH2-GRS.

We have modified the solver package T2SOLV of TOUGH2 to speed up the iterative solvers DSLUBC, DSLUCS, DLUSTB, and DSLUGM. This modification improves the transformation from coordinate format (COO) to compressed sparse column format (CSC) by changing the routines DS2Y and QS2I1D. The modified solver package was presented at the TOUGH-Symposium 2015 /NAV 15/ and has shown to yield a significant speed improvement of about 25 – 30 % /JUN 17/.

The code TOUGH2-MP-GRS, version 0, has been constructed by porting the GRS code extensions of TOUGH2-GRS to TOUGH2-MP, version 2.0.

## 2.2        Major code versions

Full version names of TOUGH2-GRS and TOUGH2-MP-GRS take the form

```
<major version>.<minor version>.<patch version>.
```

The major code version is assigned to specific code development projects. The minor version indicates weather codes are compatible. Source codes sharing the same minor version have to be compatible with regard to functionality, input and output parameters. Patch versions introduce bug-fixes or minor code changes. This report only refers to major code versions.

### TOUGH2-GRS v. 0

The main achievement of this code version was to integrate previous lines of code development into a single code. The code was developed in BMU project UM10A03200 (VSG) /NAV 13b/.

### TOUGH2-GRS v. 1

Version 01 of TOUGH2-GRS was subject to a major restructuring and benefited from a highly modular structure. New physical processes (called process modules) were added and the implementation of existing modules was substantially changed. All physical process modules (except for modules PRLIM and RN) were included in the implicit Newton-Raphson solution scheme to yield higher accuracy. Version 1 introduced non-comprehensive plausibility checks for input data as well as a reporting system for messages, warnings and errors. The code developments have been conducted in BMU project UM13A03400 (ZIESEL) /NAV 16a/.

### TOUGH2-GRS v. 2

The present version 2, which has been developed in BMU project 4715E03230, introduces new features:

- Temperature-dependent capillary pressures
- Anion exclusion for module RN
- Controls for the Burlirsch-Stoer solver of the RN module
- Irreversible softening for module FISS

The input data for porosity-dependent permeabilities and capillary pressures have moved from module COMP to the new module RELA because the related processes are not restricted to the process of compaction.

The coupling of the TOUGH2 with the geomechanical code FLAC3D, called TFC, has been a stand-alone code before. It is now part of TOUGH2-GRS and will be documented separately. Since TFC requires a serial version of TOUGH2 it will not become part of the parallel TOUGH2-MP-GRS code.

The code developments have been conducted in BMU project 4715E03230.

### TOUGH2-MP-GRS v. 0

In BMU project 4715E03230, most of the code extensions of TOUGH2-GRS have been ported to the code TOUGH2-MP /ZHA 08/. The general code structure of the ported code parts has not been changed but additional routines were implemented for the

exchange of data between processes. Read and write operations are only carried out by process 0 which requires inter-process communication for the distribution and collection of data. The RN module demands additional process communication owing to the flow calculations it performs.


## 2.3      Differences between TOUGH2 and TOUGH2-MP

Compared to TOUGH2, the code TOUGH2-MP has some divergent features /ZHA 08/:

- Zero volume elements are no longer used for the definition of inactive elements. Large-volume elements have to be used for this purpose.

- ICP = 8 now selects the ECM capillary pressure function and ICP = 9 a generalized ECM function (see /ZHA 08/ for details). On the contrary, ICP = 8 of the TOUGH2 code means "no capillary pressure".

- ICP = 9, 10 now selects the ECM function (see /ZHA 08/ for details).

- For T2R3D, an additional rock card is required with radionuclide specific transport properties.

- MOP(10): A new interpolation formula for heat conductivity has been introduced and can be selected by MOP(10)=2.

- MOP(14): This switch specifies whether 5- or 8-character elements are used. Zero stands for 5-character elements. The choice affects the length of strings for elements and connections used in the input blocks ELEME, CONNE, GENER, INCON, FOFT, COFT, and GOFT.

- MOP(15) = 1 (heat exchange) has not been implemented in TOUGH2-MP.

- MOP(17) allows to generate a file holding T2R3D transport simulations for EOS9.

- MOP(20) controls the format of CONNE and GENER indexes (0 uses format 16I5 and 1 uses format 10I8)

- If REDLT < 0 is chosen –REDLT will be used as increasing rate for time-step size.

- NELIST and EPLIST(I) are used to print time series of primary variables for selected elements.

- Card TIMBC introduces a table for time-dependent pressure boundary conditions.

- Card RTSOL introduces additional parameters for time stepping, iteration and solvers.

These features have remained unchanged in TOUGH2-MP-GRS except for the roll-back to the original ICP = 8 ("no capillary pressure") feature.

Note that TOUGH2-MP requires at least 4 elements and 3 connections.

## 2.4 Deviations from TOUGH2 and TOUGH2-MP defaults

### 2.4.1 Unlimited number of materials (only TOUGH2-GRS)

TOUGH2-GRS still uses static array sizes. The maximum number of materials can be adjusted by parameter MR, which is located in file module_sizes.f90. Note that MR has to be *larger* than the number of materials in use because of the specific coding of the TOUGH2 input routine, which has remained unchanged.

### 2.4.2 Unlimited number of time steps

Parameter MCYC determines the maximum number of time steps. The default value MCYC=0 forces TOUGH2 v. 2.0 to quit the simulation prior to the first time step. On the contrary, TOUGH2-GRS uses MCYC=0 to indicate the absence of a time step limit. Input files of TOUGH2-GRS therefore cannot be used with TOUGH2 v. 2.0 if MCYC = 0.

### 2.4.3 Automatic Leverett scaling disabled

In contrast to TOUGH2 v. 2.0 there is no automatic Leverett scaling of capillary pressures if permeability modifiers (PM) are used.

### 2.4.4 Extended printouts

TOUGH2-GRS and TOUGH2-MP-GRS generate additional printout at time zero and after the last time step. The default value of parameter `MCYPR` (`MCYPR=0`) defining the maximum time step difference between two printouts has been changed from 1 to $10^7$.

Element and connection specific printouts are directed to the output files ELE_MAIN and CON_MAIN using the data format of the time series files FOFT, COFT, and GOFT.

The printout of total component masses in active elements (the printout that starts with `"MASS IN PLACE"`) is now a printout for elements with volume smaller than 1E+50 m³.

### 2.4.5 Conservation of floating point precision (only TOUGH2-GRS)

Input data are read by TOUGH2 v. 2.0 either from the STDIN channel or from separate files like the MESH file. If input data is passed via the STDIN channel, the data will first be written to a separate file and reread afterwards. This indirect reading of input data may cause a loss of floating point precision.

Read and write operations of TOUGH2 v. 2.0 are performed using the format string "E10.4". This causes a loss of precision if the user makes efficient use of the field length. Let us consider the read and write operations for the element volume, which is stored in the ELEME data block. Reading a numerical value of 1.23456E+4 from the STDIN channel by means of the format string "E10.4" is not a problem, but writing this value to the MESH with the same format string yields 0.1235E+05 if the gfortran 4.9.3 compiler is used. Apparently, the introduction of leading zeros to the significand and exponent has resulted in a loss of two digits. TOUGH2-GRS solves this problem by reading and writing strings ("A10") instead of floating point values.

### 2.4.6 Enforced solution of linear equations

If convergence is achieved in the cycle of the Newton-Raphson iteration, primary variables remain unchanged because the linear equations are not solved. Consequently, sources and sinks (which are introduced by adding a term to the right side of the linear equation system) remain inactive. This usually is not a major problem because the convergence criteria are met. However, the absence of sinks and sources can cause

significant problems in connection with the CORFL, COMP and CORRO modules of TOUGH2-GRS, which are introducing sinks and sources. The respective processes are stalled if convergence is achieved in the first cycle and this might sum up to significant errors with time. TOUGH2-GRS and TOUGH2-MP-GRS therefore enforce at least two iterations (`ITER > 1`). The related MOP(21) switch of TOUGH2-MP-GRS has been de-activated.


## 2.5      Modules and physical processes

TOUGH2-GRS and TOUGH2-MP extensions are organized in Fortran modules as shown in Tab. 2.1. Some modules introduce new input data block named after the module's name. All modules have been developed for the use with the EOS7 and EOS7R. However, the combination TOUGH2-MP-GRS/EOS7R has not been extensively tested yet.

Fortran modules cannot use each other in a circular manner. To clarify module dependencies, modules are grouped in ten levels according to Tab. 2.1. Modules are only allowed to use modules of a lower level. The compilation of modules has to proceed from the lowest to the highest level.

Modules COMP, CORFL, CORRO, DEGRA, FISS, GCOMP, PRLIM, RELA and RN introduce new physical processes or properties. We will refer to these modules as "process modules".

Some process modules do not only change porosity but also require information on the current porosity estimation of other process modules. For this reason, variables holding porosity changes have been ported from the process modules to a separate module PORO. As a lower-level module, PORO can be accessed by every process module in order to obtain information on porosity change estimates of other process modules. The PORO module contains common routines for porosity handling as well as a routine for the reduction of connection interfaces due to compaction (see also chapter 2.6).

Permeability changes are managed differently from porosity changes because no module requires permeability estimates of other process modules. For this reason, the permeability change module PERM is a high-level module. It collects permeability changes induced by process modules and passes them to the TOUGH2 core.

**Tab. 2.1**    Fortran modules of TOUGH2-GRS and TOUGH2-MP-GRS

Modules in bold face introduce new data blocks. Data block keywords correspond to the module names.

| Level | Fortran modules of the code extension | | Purpose |
|---|---|---|---|
| | **TOUGH2-GRS** | **TOUGH2-MP-GRS** | |
| 10 | PROGFLOW | PROGFLOW | High-level routines used as an interface for the TOUGH2 and TOUGH2-MP cores |
| 9 | TEST | TEST | Plausibility tests for input data |
| | OUTPUT | OUTPUT | Extended output |
| | ANALYSE | - | Run-time monitoring for the physical interpretation of convergence failures |
| | NEWBLOCKS | NEWBLOCKS | General routines for new input data blocks |
| 8 | PERM | PERM | General permeability routines and externalized permeability variables |
| 7 | **CNTRL** | **CNTRL** | General controls including time step control |
| | **COMP** | **COMP** | Compaction of crushed salt backfill in rock salt cavities including changes of permeability and capillary pressure |
| | **CORFL** | **CORFL** | Seal corrosion by corroding fluids |
| | **CORRO** | **CORRO** | Gas production and water consumption due to metal corrosion |
| | **DEGRA** | **DEGRA** | Time-dependent change of seal permeability |
| | **DOFT** | **DOFT** | Time series for domains (rocks) |
| | **FISS** | **FISS** | Transport of gas in microscopic pathways including porosity and permeability changes, pressure thresholds, softening mechanisms and kinetic effects |
| | **GCOMP** | **GCOMP** | Properties of the main gas component of EOS7(R) |
| | **PRLIM** | **PRLIM** | Pressure limitation caused by the escape of gas from the model domain |
| | **PTIME** | **PTIME** | TIME vector with higher precision |
| | **RN** | **RN** | Decay, advection, diffusion, linear sorption and anion exclusion for radionuclide chains |
| | **RANGE** | **RANGE** | Limits primary variables |
| 6 | **RELA** | **RELA** | Functional dependencies for permeability and capillary pressure |
| 5 | PORO | PORO | General routines for porosity change and externalized porosity variables |
| 4 | ALARM | ALARM | Reporting system for messages, warnings, and errors |
| | - | TIMER | Time measurement |
| 3 | MISC | MISC | General constants and routines |
| 2 | TOUGH | MODULES | Gives access to global TOUGH2 variables |
| 1 | SIZES | *(not needed)* | Static TOUGH2 array sizes |

## 2.6        Handling porosity changes

Porosity changes that are caused by matrix compression and thermal expansion are basic parts of TOUGH2-based codes. TOUGH2-GRS and TOUGH2-MP-GRS additionally consider porosity changes induced by backfill compaction (module COMP, see chapter 4) and opening of micro fissures by the gas phase (module FISS, see chapter 9).

TOUGH2's algorithm of altering porosities is retained: At first, porosity is changed by simply setting the porosity variable PHI to the new value without touching other variables like for instance gas saturation. Changing the porosity variable in this way brings on a change of component masses, which is rectified in a second step by introducing compensating sinks or sources for the respective components. This is an efficient way to model porosity changes that are not instantaneous but coupled to flow processes.

Every Newton-Raphson iteration calculates a new porosity estimation PHI ($\phi_{\text{tough}}$). This is achieved by adding the porosity changes related to backfill compaction ($\Delta\phi_{\text{comp}}$), opening of micro-fissures ($\Delta\phi_{\text{fiss}}$), rock compaction and thermal expansion ($\Delta\phi_{\text{ce}}$)

$$\Delta\phi_{\text{tough}} = \Delta\phi_{\text{ce}} + \Delta\phi_{\text{comp}} + \Delta\phi_{\text{fiss}}$$

(2.1)

in order to obtain the porosity change $\Delta\phi_{\text{tough}}$ after the last time step.

Porosity changes due to rock compaction and thermal expansion usually are so small that consequent changes in element volume can be neglected. In contrast, porosity changes caused by backfill compaction ($\Delta\phi_{\text{comp}}$) can considerably alter the element volume. Since the TOUGH2 variable for the element volume EVOL is a constant (called $V_{\text{tough}}$ in the following) a new variable $V_{\text{phys}}(t)$ is introduced describing the physical volume of the compacting material. $V_{\text{phys}}(t)$ is accompanied by a new porosity variable for the porosity of the compacting domain $\phi_{\text{phys}}$.

The volume and porosity variables of TOUGH2, $V_{\text{tough}}$ and $\phi_{\text{tough}}(t)$, are related to the new volume and porosity variables of TOUGH2 of TOUGH2-GRS and TOUGH2-MP-GRS by the assumption of pore space conservation:

$$V_{\text{phys}}(t) \cdot \phi_{\text{phys}}(t) = V_{\text{tough}} \cdot \phi_{\text{tough}}(t)$$

(2.2)

$V_{\text{cavity}}(t)$ and $\phi_{\text{tough}}(t)$ are updated every Newton-Raphson iteration under the assumption that the change of element volume equals the change of pore volume:

$$V_{\text{cavity}}(t) = V_{\text{cavity}}(t_{\text{old}}) + V_{\text{tough}} \cdot \Delta\phi_{\text{comp}} \tag{2.3}$$

$$\phi_{\text{tough}}(t) = \phi_{\text{tough}}(t_{\text{old}}) + \Delta\phi_{\text{ce}} + \Delta\phi_{\text{comp}} + \Delta\phi_{\text{fiss}}, \tag{2.4}$$

where $t_{\text{old}}$ is the time after the last successful time step.

By definition, fissure porosity $\phi_{\text{fiss}}$ is only accessible to gas (see chapter 9) so that capillary pressures should vanish if the liquid-accessible porosity $\phi_{\text{phys}} - \phi_{\text{fiss}}$ is saturated. Capillary pressure functions of TOUGH2-GRS and TOUGH2-MP-GRS therefore depend on the liquid saturation not of the total but of the liquid-accessible porosity $\hat{S}_{\text{liq}}$. The liquid-accessible porosity is

$$\hat{S}_{\text{liq}} = S_{\text{liq}} \cdot \left(1 - \frac{\phi_{\text{fiss}}}{\phi_{\text{phys}}}\right)^{-1}, \tag{2.5}$$

which is derived from the relation

$$S_{\text{liq}} \cdot \phi_{\text{phys}} \cdot V_{\text{phys}} = \hat{S}_{\text{liq}} \cdot (\phi_{\text{phys}} - \phi_{\text{fiss}}) \cdot V_{\text{phys}} \tag{2.6}$$

Large changes of porosity and element volume should also be considered in the flow section of element connections. Changing interface areas would require the introduction of a separate weighting scheme for volume changes, since the latter are connected to elements. We avoid introducing a separate weighting scheme by modifying permeabilities, diffusivities, and thermal conductivities of elements instead. All of these variables variables are multiplied by a correction factor

$$\frac{A_t}{A_0} \tag{2.7}$$

with $A_0$ being the interface area of the connection and $A_t$ the true interface area at time $t$. To calculate $A_t/A_0$ we assume that rock convergence is the chief contributor to volume change and that drifts are the most important structures to be considered. Convergence of a drift takes place in two dimensions so that we can set

$$\frac{A_t}{A_0} = \frac{V_t}{V_0} \, , \tag{2.8}$$

where $V_0$ is the initial element volume and $V_t$ is the true volume at time $t$. Note that this relation is based on the above-mentioned assumptions.

## 2.7        Handling permeability changes

Modules DEGRA and CORFL introduce time-dependent changes of intrinsic permeability by means of the permeability factors $f_{\mathrm{DEGRA}}$ and $f_{\mathrm{CORFL}}$, respectively. If defined, the isotropic porosity-permeability relation $k_{\mathrm{RELA}}(\phi)$ of module RELA substitutes the anisotropic permeability $\vec{k}_{\mathrm{ROCKS}}$ of data block ROCKS:

$$\vec{k} = \begin{cases} |f_{\mathrm{PM}}| f_{\mathrm{DEGRA}}\, f_{\mathrm{CORFL}}\, k_{\mathrm{RELA}}(\phi)\,\mathbf{I} & \text{if } k_{\mathrm{RELA}}(\phi) \text{ is defined and } f_{\mathrm{PM}} \geq 0 \\ |f_{\mathrm{PM}}|\, f_{\mathrm{DEGRA}}\, f_{\mathrm{CORFL}}\, \vec{k}_{\mathrm{ROCKS}} & \text{otherwise} \end{cases} \tag{2.9}$$

Permeability modifiers $f_{\mathrm{DEGRA}}$ and $f_{\mathrm{CORFL}}$ are set to 1 if the respective module is inactive. $f_{\mathrm{PM}}$ is the TOUGH2 permeability modifier PM of data block ELEME. In equation (2.9), we use the absolute value of $f_{\mathrm{PM}}$ because the RELA module uses negative values of $f_{\mathrm{PM}}$ as a switch to turn off the porosity-permeability relationship $k_{\mathrm{COMP}}(\phi)$ for single elements.

Module FISS introduces a new permeability term to the flow equation of the gas phase without changing intrinsic permeability $\vec{k}$. This is explained in chapter 10, see equation (10.14) on p. 49.

# 3 New flow and transport features

## 3.1 Check valve boundary (IRP=9 in combination with an upstream weighting of mobilities)

Flow boundaries can be designed as one-way outlets (a check valve behaviour) by defining inactive elements with zero permeability. However, this approach works only if intrinsic permeabilities are upstream-weighted. With harmonic weighting a vanishing permeability no advective flow would be possible.

In connection with a harmonic weighting of permeabilities, one-way outlets can now be introduced by choosing upstream weighted mobilities (`MOP(11)= 2`) and applying the new permeability function `IRP = 9` to inactive elements. `IRP = 9` sets the relative permeability to zero for all phases, so that fluids can only flow into the boundary but not leave it.

## 3.2 Simulated vertical pressure gradient (ICP=9 with IRP=1)

If the host rock of a repository is impermeable rock salt it usually does not have to be included in the modelling grid. Consequently, the modelling grids for such repositories usually are networks of mining cavities, namely drifts, chambers and shafts.

Acceptable simulation times for repositories in rock salt can often be achieved by a coarse spatial discretization. One possibility to do so is to model horizontal drifts as one-dimensional structures without vertical discretization. This approach saves computation time but has to be used with caution because it can introduce the wrong physics.

Without vertical discretization no gravitational flow takes place. Consequently, the gas phase is unable to ascend to the top of the drift but remains distributed homogeneously in vertical direction. The hydraulic behaviour of such a system can differ significantly from systems with gravitational flow that allow for a vertical separation of phases. Let us consider the case of a gas bubble that has been trapped in front of a gastight seal. If vertical phase separation is possible, the gas bubble ascends and accumulates at the top of the drift, allowing the liquid phase pass by. In contrast, without vertical phase separation, the gas phase remains homogeneously distributed thereby blocking the flow of liquid through the seal.

However, it is still possible to simulate a vertical separation of phases within drifts even if there is no vertical discretisation. This can be achieved by substituting the missing gravitational forces by capillary forces. TOUGH2-GRS and TOUGH2-MP-GRS introduce a new capillary pressure function (`ICP = 9`), which adds a correction term to the van Genuchten capillary pressure function. The purpose of the correction term is to compensate for the lack of gravitational forces that is caused by the missing vertical discretisation.

To derive the correction term we examine the two flow systems shown in Fig. 3.1. Both systems are closed systems with constant initial gas pressure and no capillary forces. System A is composed of two grid elements with gas saturation $S_{g1}$ and $S_{g2}$. System B is derived from system A by subdividing the elements in vertical direction. The mean gas saturation of domain 1 and 2 in system B shall be equal to the gas saturation of element 1 and 2 in system A, respectively.
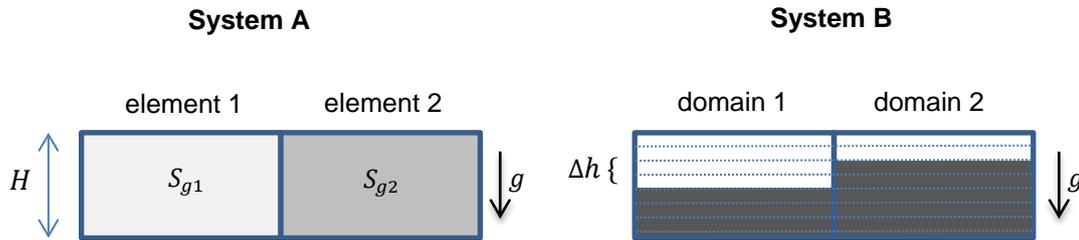


**Fig. 3.1**     Models for drift sections with (A) and without (B) vertical discretisation

$g$: gravity, $H$: drift height, $\Delta h$: height difference of water columns, $S_g$: gas saturation.

System B establishes a liquid flow from domain 2 to domain 1 because of the pressure difference

$$\Delta p_{2\to 1} = -\varrho g \Delta h \left(S_{\mathrm{g2}} - S_{\mathrm{g1}}\right)$$

(3.1)

induced by the height difference of both water columns (note that $S_{\mathrm{g1}}$ and $S_{\mathrm{g2}}$ refer to a gas and not to a liquid saturation). Here, $\varrho$ is the liquid density, $g$ the gravitational acceleration and $\Delta h$ the height difference between the water columns.

In contrast to system B, system A will not establish a liquid flow because of the equality of pressures at the element centres. To initiate the same flux as in system B, a correction pressure

$$p_{\mathrm{grav}}(S_g) := -\varrho g H S_g$$

(3.2)

has to be introduced, which leads to the desired pressure difference

$$\Delta p_{\mathrm{grav},2\to1} = -\varrho g \Delta h \left(S_{\mathrm{g2}} - S_{\mathrm{g1}}\right).$$

(3.3)

We add the correction pressure to the capillary pressure function $p_{\mathrm{cap}}(S_g)$ to yield a corrective capillary pressure

$$\hat{p}_{\mathrm{cap}}(S_g) = p_{\mathrm{cap}}(S_g) + p_{\mathrm{grav}}(S_g),$$

(3.4)

which compensates for the missing gravitational effects in drifts without vertical discretisation (Note that TOUGH2 uses negative capillary pressures). If $p_{\mathrm{cap}}(S_g)$ is the van Genuchten function /GEN 80/, $\hat{p}_{\mathrm{cap}}$ can be selected by setting `ICP` = 9. The input parameters `CP(1)` to `CP(5)` are the same as for the van Genuchten function (`ICP` = 7). The additional parameter `CP(6)` holds the term $\varrho g H$.

To account for the linear dependency between the flow section and saturation a linear relationship for the relative permeabilities should be used (`IRP` = 1), see /NAV 16b/.

# 4        CNTRL: Simulation controls

The CNTRL module holds various simulation controls related to termination criteria, automatic time stepping, and printing. The structure of data block CNTRL is shown in Tab. 4.1.

## 4.1        Termination controls

### 4.1.1        Do not exit on equilibrium (obsolete)

TOUGH2 v. 2.0 uses two criteria for the detection of static or dynamic equilibria. The code terminates if either ten iterations with `ITER`=1 have occurred or if there is a convergence failure after two subsequent iterations with `ITER`=1. Since version 00 of TOUGH2-GRS, the CNTRL module allows to disable these criteria by means of the two parameters `cntrl_ignore10TimesIterEq1` and `cntrl_ignoreConvFailureAfter2TimesIterEq1`. However, this feature has become obsolete since TOUGH2-GRS v. 01 due to the enforcement of at least two iterations (see chapter 2.4.6).

### 4.1.2        Minimum time step width

Some process modules can induce high fluxes. The CORFL module, for instance, can trigger rapid flow processes after seal failure. Fast processes usually cause a drastic reduction of time step widths to a degree where simulations become inefficient and should be terminated. To avoid stagnant simulations with unreasonably small step widths, the parameters `minStepSize` and `stopAfter` can be used terminate the execution as soon as the time step width falls below `minStepSize` for `stopAfter` successive time steps.

## 4.2        Time step controls

### 4.2.1        Incrementing step widths

TOUGH2 increases time step widths if the number of Newton-Raphson iterations `ITER` is smaller than or equal to `MOP(16)`. The standard increasing factor is 2 but can now be adjusted by means of parameter `dtfacQuickIter`.

The fact that TOUGH2 stops to increase step widths if `ITER > MOP(16)` means that the bandwidth of time steps meeting the criterion `NOITE ≥ ITER > MOP(16)` is not sufficiently explored. The automatic time stepping control of TOUGH2 works fine if this bandwidth remains small. However, there are cases where the bandwidth is large and should be explored by the automatic time stepping control. This can now be achieved by setting parameter `dtfacSlowIter` with 1 ≤ `dtfacSlowIter` < `dtfacQuickIter`. Parameter `dtfacSlowIter` is the increasing factor for time step widths in case of `NOITE ≥ ITER > MOP(16)`.

### 4.2.2        Avoiding convergence failures

If the bandwidth of time steps meeting the criterion `NOITE ≥ ITER > MOP(16)` is too small or even zero, the performance of the simulation will suffer from too many convergence failures. In order to avoid this, TOUGH2-GRS and TOUGH2-MP-GRS can be instructed to avoid the last time step width that has produced a convergence failure for at least `cntrl_avoiddt` time steps.

### 4.2.3        Avoiding small time steps before printout times

Printout times introduced by data blocks TIMES and PTIMES can lead to a drastic reduction of time step widths because overshooting time steps have to be clipped in order to reach the specified printout time.

Setting `cntrl_softlanding` = 1 activates an automatic step width adjustment to attenuate this effect. If activated, it is checked whether the next printout time is nearer than a quadruple of the current time step size and if so, the step width is slightly reduced with the aim of dividing the time to the next printout into four almost equal parts.

### 4.2.4 Avoiding large changes in gas generation

If sinks and sources are introduced using interpolated tabular data (`MOP(12)=0`) large time steps can lead to an inaccurate mass injection or production. Setting parameter `cntrl_MaxRelGenRateChange` to a positive value reduces the time step width in a way that changes of generation rates remain smaller than parameter `cntrl_MaxRelGenRateChange` (rate change per rate).

### 4.3 Output controls

### 4.3.1 Precision of time series printouts

Data blocks FOFT, COFT and GOFT introduce time series printouts for specified elements, connections, and sources, respectively. TOUGH2-GRS and TOUGH2-MP-GRS introduce additional domain-specific printouts by means of data block DOFT (see chapter 16.6).

Time series printouts can be very large if there are a lot of time steps. The file size can be controlled by parameter `cntrl_decimalplaces`, which adjusts the number of decimal places. (Note that values of 0 and 1 will always be printed as "0." and "1.", respectively, no matter how many decimal places are prescribed.) A negative value of `cntrl_decimalplaces` converts the printout to binary format using the output files `FOFT.bin`, `COFT.bin`, `GOFT.bin`, and `DOFT.bin`. These files can be converted to ASCII format by means of the tool `translate.f90`.

### 4.3.2 Reducing the amount of time series printouts

An effective way of decreasing the size of time series printouts is to skip time steps. Parameter `cntrl_ioft` defines a minimum time step difference between successive printouts. Parameter `cntrl_MinRelDur` multiplied by the current time gives the minimum time between successive printouts.

## 4.4 Input data

Tab. 4.1 shows the structure of data block CNTRL.

**Tab. 4.1** Input format of data block CNTRL

| Line | Column | Content | Format | Unit | Description | Variables (Long names! Ignore line feeds.) |
|------|--------|---------|--------|------|-------------|--------------------------------------------|
| 1 | 1-5 | `"CNTRL"` | A5 | | Keyword | |
| w2 | 1-10 | Do not stop after 10 iterations with ITER=1? | I10 | | 0: no<br>1: yes | `cntrl_ignore10TimesIterEq1` |
| 2 | 11-20 | Do not stop after convergence failure subsequent to two iterations with ITER=1? | I10 | | 0: no<br>1: yes | `cntrl_ignoreConvFailureAfter2TimesIterEq1` |
| 3 | 1-10 | Stop execution if time step width remains N times below Tmin? | G10.4 | sec | Tmin (inactive if equal 0) | `minStepSize` |
| 3 | 11-20 | | I10 | | N | `stopAfter` |
| 4 | 1-10 | Factor for the increase of time step width if ITER < MOP(16) | G10.4 | | default: 2<br>recommended: 1.2 | `cntrl_dtfacQuickIter` |
| 4 | 11-20 | Factor for the increase of time step width if ITER >= MOP(16) | G10.4 | | default: 1<br>recommended: 1.1 | `cntrl_dtfacSlowIter` |
| 5 | 1-10 | Number of time steps that avoid last time step width with convergence failure | I10 | | 0: inactive | `cntrl_avoiddt` |
| 6 | 1-10 | Adapt time stepping in order to avoid small time step widths before printout times | I10 | | 0: no<br>1: yes | `cntrl_softlanding` |
| 7 | 1-10 | Maximum relative change of the generation rate if linear interpolated tables are used (rate change per rate) | G10.4 | | 0: inactive | `cntrl_MaxRelGenRateChange` |
| 8 | 1-10 | Decimal places of real numbers | I10 | | 0: switches to 12,<br><0: binary output | `cntrl_decimalplaces` |
| 9 | 1-10 | Stride for time series printouts (FOFT, COFT etc.) | I10 | | 0: switches to 1 (=print every time step) | `cntrl_ioft` |
| 10 | 1-10 | Minimum time between two time series printouts divided by time | G10.4 | | 0: inactive | `cntrl_MinRelDur` |
| 11 | 1-10 | Printout run-time information to STDOUT (not in use anymore) | I10 | | 0: no<br>1: yes | `cntrl_monitoring` |

# 5 COMP: Convergence and compaction

Rock salt is subject to creep deformation. Mining cavities in rock salt therefore contract with time. This process is usually called "convergence" because the walls of a spherical cavity tend to converge against one point. The rate of convergence depends on the support of the backfill, if present, but also on the fluid pressure within the cavity. Convergence compresses the backfill and reduces its porosity as well as its permeability. Capillary pressures and relative permeabilities may change too.

The COMP module implements the combined process of convergence and backfill compaction. The mathematical model will only be described briefly in this report. Further details on the origin and purpose of the model can be found in /NAV 13c/ in German language.

## 5.1 Physical models

### 5.1.1 Change of cavity volume and porosity

According to /STE 85/ the volume change of a cavity with volume $V(t)$ due to convergence can be described by the differential equation

$$\dot{V}(t) = -K \cdot V(t) \tag{5.1}$$

Factor $K > 0$ is called the rate of convergence and depends on the local pressure, porosity, and temperature. Volume $V$ is the volume of an entire cavity and is not to be confused with the volume of grid elements used for the discretisation of that cavity. However, if a homogeneous distribution of $K$ in the backfill is assumed, equation (5.1) also describes the compaction of a subvolume $i$ of the cavity (a grid element, for example):

$$\dot{V}_i = -K \cdot V_i \quad \text{with} \quad \sum_i V_i = V. \tag{5.2}$$

Factor $K$ of equation (5.2) does not refer to the convergence of a cavity anymore but to the convergence of a grid element, which is part of a converging cavity. We therefore

call $K$ of equation (5.2) a *rate of compaction*, not a rate of convergence. TOUGH2-GRS and TOUGH2-MP-GRS apply equation (5.2) using the physical volume variable described in chapter 2.6.

## 5.1.2 Compaction rates

Compaction rates are calculated using a slightly modified approach of /NOS 05/. In /NAV 13c/, this approach is called the "extended approach of Stelte". Here, the convergence rate is derived from a *reference convergence rate* $K_{ref}$ by applying factors for the dependencies of the convergence rate on location, pressure, backfill porosity, time, and temperature. (Note that we set compaction rates equal to convergence rates.)

$$K = \begin{cases} K_{ref} \cdot f_{loc} \cdot f_p \cdot f_\phi \cdot f_t \cdot f_T & \text{for} \quad \phi > \phi_{lim} \\ 0 & \text{for} \quad \phi \leq \phi_{lim} \end{cases} \quad (5.3)$$

Variable $\phi_{lim}$ is a lower porosity limit, which is not part of the extended approach of Stelte. The factors of the term belonging to $\phi > \phi_{lim}$ are the following.

- **Reference convergence rate.** It has been assumed by Stelte that the convergence rate of an open cavity converges against a constant value, the *stationary convergence rate* /NAV 13c/. The reference convergence rate $K_{ref}$ is the stationary convergence rate of an open cavity at reference conditions $p_{ref} = 1$ bar (the reference gas pressure in the cavity) and $T_{ref}$ (the temperature of the surrounding rock). The reference convergence rate can be estimated from in-situ measurements or geomechanical simulations.

- **Local dependency.** $f_{loc}$ captures spatial dependencies of the stationary convergence rate. The stationary convergence rate usually varies with depth, temperature, and geometry of the cavity.

- **Pressure dependency.** The convergence rate of a cavity decreases with increasing pore pressure. Assuming isotropic stress $p_G$ in the surrounding rock, the dependency on the mean pore pressure $\hat{p}$ is described by a factor

$$f_p = \left(1 - \frac{\hat{p} - p_{ref}}{p_G - p_{ref}}\right)^{m_p} \quad \text{for} \quad p \leq p_G, \quad \text{otherwise } f_p = 0. \quad (5.4)$$

$p_G$ is the isotropic lithostatic pressure that would have been present at the reference location in the absence of a cavity. The mean pore pressure $\hat{p}$ is calculated as the

arithmetic mean of gas pressure $p_{gas}$ and liquid pressure $p_{liq}$ weighted by the liquid saturation $S_{liq}$ in the following way.

$$\hat{p} = p_{gas}(1 - S_{liq}) + p_{liq}S_{liq} = p_{gas} + p_{cap}S_{liq} \tag{5.5}$$

Note that the variation of $p_G$ with depth is not covered by this approach.

- **Backfill support.** The supporting pressure on the cavity walls caused by the backfill increases with increasing compaction. The factor

$$f_\phi(\phi, \phi_r) = \left[1 + \frac{h(\phi, \phi_r)}{(\phi \cdot g(\phi, \phi_r))^{1/m_\phi}}\right]^{-m_\phi} \quad \text{for} \quad \phi < \phi_r, \text{ otherwise } f_\phi = 1, \tag{5.6}$$

describes the influence of the supporting pressure on the convergence rate, where $\phi_r$ is the porosity at the onset of the supporting pressure. Functions $h(\phi, \phi_r)$ and $g(\phi, \phi_r)$ are approximated by

$$h(\phi, \phi_r) = h_0 + h_1\frac{\phi}{\phi_r} + h_2\left(\frac{\phi}{\phi_r}\right)^2 + h_3\left(\frac{\phi}{\phi_r}\right)^3 \text{ and} \tag{5.7}$$

$$g(\phi, \phi_r) = g_0 + g_1\frac{\phi}{\phi_r} + g_2\left(\frac{\phi}{\phi_r}\right)^2 \tag{5.8}$$

with $h_0 = 1$, $h_2 = -(3 + 2h_1)$, $h_3 = h_1 + 2$ and $g_0 = 1$. Parameters $\phi_0$, $h_1$, $g_1$, and $g_2$ are input parameters. Presently, we set $m_\phi = m_p$.

- **Transient processes.** After excavation, the convergence rate of an open cavity converges against a stationary convergence rate, namely against the reference convergence rate $K_{ref}$. The gradual transition to the stationary convergence rate is expressed by the factor $f_t$

$$f_t = 1 + \frac{1}{1 + \lambda_s^{-1}\ln(V_0/V)}\left(\frac{K_0}{K_{ref} \cdot f_\phi(\phi_0)} - 1\right). \tag{5.9}$$

$K_0$ and $\phi_0$ are the initial convergence rate and initial porosity, respectively, at the start of the simulation. Parameter $\lambda_s$ chiefly depends on time and has to be determined by geomechanical calculations. For more details see /NOS 05/ and /NAV 13c/.

- **Temperature dependency.** Temperature has a strong influence on salt creep and thus on the convergence rate. Temperature dependency is captured by the factor

$$f_T(T) = \frac{1}{1+a} \cdot \exp\left(\frac{Q_1}{R} \cdot \left(\frac{1}{T_{\mathrm{ref}}} - \frac{1}{T}\right)\right) + \frac{a}{1+a} \cdot \exp\left(\frac{Q_2}{R} \cdot \left(\frac{1}{T_{\mathrm{ref}}} - \frac{1}{T}\right)\right). \qquad (5.10)$$

The equation considers two creep processes with activation energies of $Q_1$ and $Q_2$ and a weighting parameter $a$. Variable $T_{\mathrm{ref}}$ is the reference temperature, that is to say the temperature of the rock at the time of measuring the reference convergence rate. $T$ is the present temperature of the rock and $R$ the universal gas constant. The equation is only valid for a homogeneous distribution of temperature.

## 5.2        Note on the compaction of saturated media

The compaction process can cause numerical problems if a fully liquid-saturated medium is compacted under undrained or nearly undrained conditions and if the compressibility of the rock is low. Under these conditions, pressure may rise quickly and cause a drastic decrease of time step width.

## 5.3        Input data

The module introduces the new input data block COMP (see Tab. 5.1). Parameters have to be input separately for each material. However, modification of single elements is possible via the permeability modifier PM of data Block ELEME. Setting PM to a negative value disables compaction of the respective element. In the following calculations, the absolute value of PM is used as permeability modifier.

Up to TOUGH2-GRS version 1, functions for porosity-dependent permeabilities and capillary pressures had to be introduced by means of the COMP module. In order to achieve downward compatibility, these functions are still part of the COMP data block, but the respective entries (line 5 to 8) are overruled by the corresponding input data of data block RELA. For this reason, these functions are described in chapter 14.4.

**Tab. 5.1** Input format of data block COMP

| Line | Column | Content | Format | Unit | Description | Variable |
|------|--------|---------|--------|------|-------------|----------|
| 1 | 1-5 | `"COMP"` | A5 | | Keyword | |
| 2 | 1-5 | Material name | A5 | | Name of compacting material (as defined in ROCKS) In the following, `M` is the material index. | |
| 3 | 1-10 | $K_{\mathrm{ref}}$ | G10.4 | sec$^{-1}$ | Reference convergence rate | `COMP_KREF(M)` |
| | 11-20 | $f_{\mathrm{loc}}$ | G10.4 | 1 | Local modification of the reference convergence rate | `COMP_FLOC(M)` |
| | 21-30 | $p_{\mathrm{G}}$ | G10.4 | Pa | Lithostatic pressure at the location if no cavity would exist | `COMP_PG(M)` |
| | 31-40 | $m_p = m_\phi$ | G10.4 | 1 | Exponent for the calculation of $f_p$ | `COMP_M(M)` |
| | 41-50 | $\phi_{\mathrm{r}}$ | G10.4 | 1 | Porosity at which backfill support commences | `COMP_PHIref(M)` |
| | 51-60 | $h_1$ | G10.4 | 1 | Parameter for the calculation of $f_\phi$ | `COMP_H1(M)` |
| | 61-70 | $g_1$ | G10.4 | 1 | Parameter for the calculation of $f_\phi$ | `COMP_G1(M)` |
| | 71-80 | $g_2$ | G10.4 | 1 | Parameter for the calculation of $f_\phi$ | `COMP_G2(M)` |
| 4 | 1-10 | $\lambda_s$ | G10.4 | 1 | Parameter for the calculation of $f_T$ | `COMP_LAMBDAS(M)` |
| | 11-20 | $K_0$ | G10.4 | sec$^{-1}$ | Initial convergence rate | `COMP_K0(M)` |
| | 21-30 | $a$ | G10.4 | 1 | Weighting factor for creep processes | `COMP_A(M)` |
| | 31-40 | $Q_1$ | G10.4 | J/mol | Activation energy for creep process 1 | `COMP_Q1(M)` |
| | 41-50 | $Q_2$ | G10.4 | J/mol | Activation energy for creep process 2 | `COMP_Q2(M)` |
| | 51-60 | $T_{\mathrm{ref}}$ | G10.4 | °C | Temperature of the rock at the reference location | `COMP_TGREF(M)` |
| | 61-70 | $\phi_{\mathrm{lim}}$ | G10.4 | 1 | Lower porosity limit for the convergence process (may be 0) | `COMP_PHIMIN(M)` |
| 5 | 1-10 | 0 or 1 | I10 | 1 | Enable Leverett scaling of capillary pressures? (0 = no, 1 = yes) | `COMP_LEVQ(M)` |
| | 11-20 | $k_0$ | G10.4 | m² | Reference permeability for Leverett scaling | `COMP_LEVPERREF(M)` |
| | 21-30 | $\phi_0$ | G10.4 | 1 | Reference porosity for Leverett scaling | `COMP_LEVPHIREF(M)` |
| | 31-40 | $\alpha$ | G10.4 | 1 | Exponent of the Leverett scaling | `COMP_LEVEXP(M)` |
| 6 | 1-10 | $\phi_{k=0}$ | G10.4 | 1 | Permeability will be 0 for porosities $\leq \phi_{k=0}$ | `COMP_CUTOFF(M)` |
| 7 | 1-10 | $n_{\mathrm{sec}}$ | I10 | 1 | Number of subsections of the porosity-permeability relation | `COMP_NBRANCH(M)` |
| 8 | 1-10 | $a_i$ | G10.4 | m² | Factor of power law $i$ | `COMP_PERA(I,M)` |
| | 11-20 | $b_i$ | G10.4 | m² | Exponent of power law $i$ | `COMP_PERB(I,M)` |
| *Repeat line 8 for all $n_{\mathrm{sec}}$ sections* | | | | | | |
| *Repeat line 2 to 7+$n_{\mathrm{sec}}$ for all compacting materials* | | | | | | |

# 6    CORFL

The CORFL module simulates permeability changes of technical barriers (seals) caused by percolating corrosive solutions. Although originally designed for the simulation of salt concrete corrosion by magnesium bearing solutions the module has no restrictions with regard to the underlying chemistry of the seal and percolate.


## 6.1    Implementation

The CORFL module uses the primary variable *brine mass fraction* to store information on the corrosion capacity of the fluid. The brine mass fraction of *normal corrosive brine* (this term will be defined below) and non-corrosive brine is specified by the input parameters $\tilde{X}_b$ and $\hat{X}_b$. In the following we assume $\tilde{X}_b < \hat{X}_b$ indicating that the brine mass fraction increases during the corrosion process. However, the CORFL module also accepts $\tilde{X}_b > \hat{X}_b$.

If a corrosive fluid with brine mass fraction $X_b$ enters a corrodible grid element, the CORFL module changes the composition of the brine to that of non-corrosive brine, that is to brine mass fraction $\hat{X}_b$. Thus, downstream elements are not corroded. The physical assumption behind this model is a quick corrosion process causing a sharp corrosion front.

In order to raise the brine mass fraction inside a corroding element from $X_b$ to $\hat{X}_b$, the CORFL module places a brine source and a water sink at the grid element. The source and the sink are adjusted so that the change of brine composition is an isovolumetric process. This is necessary to maintain constant pore pressures during the corrosion process.

The cumulative brine mass that has been released from a seal element until time $t$ determines its degree of corrosion. The degree of corrosion is 0 for non-corroded materials and 1 for full corrosion. The permeability of a material changes in response to its degree of corrosion.

## 6.2        Source and sink calculation

The introduced brine sources and water sinks are corrected in every Newton-Raphson iteration. If the brine inside a corroding element has a brine mass fraction of $X_b \neq \hat{X}_b$ the brine source and water sink of that element must be adapted in order to achieve $X_b = \hat{X}_b$. The method for doing so is to first calculate the brine and water mass that should be present at $X_b = \hat{X}_b$ and then to add or subtract the missing or excessive masses to the source and sink. If $m_b$ is the brine mass of the current Newton-Iteration and $\hat{m}_b$ the brine mass required for $X_b = \hat{X}_b$, the brine source is corrected in this Newton-Iteration by adding the term

$$\frac{\hat{m}_b - m_b}{V\,\Delta t} \tag{6.1}$$

where $V$ is the element volume and $\Delta t$ is the time step. The current brine mass $m_b$ can be calculated from the secondary variables (PAR array) of TOUGH2

$$m_b = V \cdot \phi \cdot S_l \cdot \rho_l(X_b) \cdot X_b \tag{6.2}$$

with porosity $\phi$, liquid saturation $S_l$, liquid density $\rho_l$, and the current brine mass fraction $X_b$.

Since the change of brine mass fraction must not affect the liquid volume, the product $V \cdot \phi \cdot S_l$ has to remain constant. The intended brine mass

$$\hat{m}_b = V \cdot \phi \cdot S_l \cdot \rho_l(\hat{X}_b) \cdot \hat{X}_b \tag{6.3}$$

therefore refers to $V \cdot \phi \cdot S_l$ with $\rho_l(\hat{X}_b)$ being the liquid density at $X_b = \hat{X}_b$. Liquid density $\rho_l(\hat{X}_b)$ can be calculated using the formula implemented in the equation-of-state modules EOS7 and EOS7R, which refers to the density of pure water $\rho_w$:

$$\rho_l(X_b) = \frac{\rho_w d}{d(1 - X_b) + X_b} \tag{6.4}$$

with

$$d = \frac{\rho_b(p_0, T_0)}{\rho_w(p_0, T_0)} \tag{6.5}$$

being the ratio between the density of the reference brine $\rho_b$ and the density of pure water $\rho_w$ at reference conditions $p_0$ and $T_0$.

To avoid calculating the density of pure water, $\rho_w$ is substituted by applying equation (6.4) to the brine densities $\hat{X}_b$ and $X_b$

$$\rho_l(\hat{X}_b) = \rho_l(X_b) \frac{1 - X_b + \frac{X_b}{d}}{1 - \hat{X}_b + \frac{\hat{X}_b}{d}}. \tag{6.6}$$

Combining this equation with equation (6.3) allows to calculate the intended brine mass by means of the given primary and secondary variables of TOUGH2:

$$\hat{m}_b = V\phi S_l \rho_{liq}(X_b) \frac{1 - X_b + \frac{X_b}{d}}{1 - \hat{X}_b + \frac{\hat{X}_b}{d}} \hat{X}_b. \tag{6.7}$$

The same procedure is used to calculate the intended water mass

$$\hat{m}_w = V \cdot \phi \cdot S_l \cdot \rho_l(\hat{X}_b) \cdot (1 - \hat{X}_b), \tag{6.8}$$

which leads to

$$\hat{m}_w = V\phi S_l \rho_{liq}(X_b) \frac{1 - X_b + \frac{X_b}{d}}{1 - \hat{X}_b + \frac{\hat{X}_b}{d}} (1 - \hat{X}_b). \tag{6.9}$$

## 6.3      Degree of corrosion

The *corrosion potential* $\gamma$ is defined as the ratio between the volume of corroded solid and the liquid volume necessary for its complete corrosion. In our model, the reference liquid for the definition of the corrosion potential is a liquid, which we call which we call *normal corrosive brine* and which is characterized by a brine mass fraction of $\tilde{X}_b$.

If $V$ is the volume of a grid element and $\phi$ its porosity, $V(1 - \phi)$ is the solid volume and $V\phi$ the pore volume. If full liquid saturation is considered, we obtain the number of times the pore fluid must be exchanged for complete corrosion by

$$n = \frac{V(1-\phi)}{V\phi\ \gamma}\ . \tag{6.10}$$

Corrosion takes place if corrosive liquid with brine mass fraction $\tilde{X}_b$ and brine mass $m_b$ infiltrates. Raising the brine mass fraction from $\tilde{X}_b$ to $\hat{X}_b$ (and brine mass from $m_b$ to $\hat{m}_b$) a brine mass of $\hat{m}_b - m_b$ has to be injected. Equation (6.9) shows that a complete corrosion of the solid requires a brine mass injection of

$$m_{b,\max} = n(\hat{m}_b - m_b) = nV\phi S_l \rho_l(\tilde{X}_b)\left(\frac{1 - \tilde{X}_b + \dfrac{\tilde{X}_b}{d}}{1 - \hat{X}_b + \dfrac{\hat{X}_b}{d}}\hat{X}_b\ -\tilde{X}_b\right). \tag{6.11}$$

If $m_{b,\mathrm{sum}}(t)$ is the brine mass released by a brine source until time $t$, the degree of corrosion $g(t)$ of the grid element is

$$g(t) = \frac{m_{b,\mathrm{sum}}}{m_{b,\max}}\ . \tag{6.12}$$

## 6.4      Permeability change

We adopt the physical model of /BFS 09/ (p. 154 ff) for the permeability change of corroding seals. The model assumes a sharp, planar corrosion front migrating through the grid element due to a homogenous percolation of the seal. The corrosion front separates fully corroded material from material without any corrosion. Kinetic effects that could smoothen out the corrosion front are neglected. Note that this model might not capture the true physics of seal corrosion for all types of seals especially if seal percolation and corrosion are highly localized.

Due to the assumption of a sharp corrosion front, the degree of corrosion $g$ denotes the corroded fraction of a grid element. We keep permeability unchanged if $g = 0$. In case of $g = 1$, permeability is multiplied by a factor of $10^{\varepsilon_k}$. For a partly corroded material we assume a series connection of corroded and non-corroded material which yields

$$f_{\mathrm{CORFL}} = \frac{1}{1 - g(1 - 10^{-\varepsilon_k})} \tag{6.13}$$

for the permeability modifier $f_{\mathrm{CORFL}}$. See chapter 2.7 for details on how $f_{\mathrm{CORFL}}$ is used to modify the intrinsic permeability of a grid element.

## 6.5 Input data

Tab. 6.1 summarizes the input parameters of the CORFL module. All corrosion parameters are material-specific.

**Tab. 6.1** Input format of data block CORFL

| Line | Column | Content | Format | Unit | Description | Variable |
|------|--------|---------|--------|------|-------------|----------|
| 1 | 1-5 | `"CORFL"` | A5 | | Keyword | |
| 2 | 1-5 | material name | A5 | | Name of compacting material (as defined in ROCKS)<br>In the following, `M` is the material index. | |
| 3 | 1-10 | $\gamma$ | G10.4 | 1 | Corrosion potential<br>(volume of solid corroded per solute volume) | `CORFL_UK(M)` |
| | 11-20 | | | | *unused* | |
| | 21-30 | $\tilde{X}_{\mathrm{b}}$ | G10.4 | 1 | Brine mass fraction of corrosive brine<br>(choose brine used in corrosion experiment in order to determine corrosion potential) | `CORFL_XB1(M)` |
| | 31-40 | $\hat{X}_{\mathrm{b}}$ | G10.4 | 1 | Brine mass fraction of non-corrosive brine<br>(choose $\hat{X}_{\mathrm{b}} \neq \tilde{X}_{\mathrm{b}}$) | `CORFL_XB2(M)` |
| | 41-50 | | | | *unused* | |
| | 51-60 | $\varepsilon_{\mathrm{k}}$ | G10.4 | 1 | Permeability factor of fully corroded element is $10^{\varepsilon_{\mathrm{k}}}$ | `CORFL_EK(M)` |
| | | | | | *Repeat line 2 to 3 for all corroding materials* | |

# 7 CORRO: Gas production due to iron corrosion

In repositories for radioactive waste, corrosion of iron is an important gas source. Iron corrosion requires the presence of water and consequently that the availability of water can become a limiting factor for gas production. Water-dependent iron corrosion can be simulated by the CORRO module by introducing gas sources and liquid sinks.

Gas sources are characterized by a gas generation rate (mole per second) and a maximum amount of produced gas. Gas sources can be either placed inside a grid element or distributed over a material domain assuming equal gas generation rate per element volume within the domain.

Gas sources can be specified as water consuming sources. In this case, gas production is limited to the availability of water. The rate of water consumption is coupled to the rate of gas production by the ratio $r_{w/g}$ (`CORRO_moleWaterPerMoleGas`), which describes how many mole of water are consumed for every mole of gas that is produced.

Each gas source becomes inactive as soon as the maximum amount of gas has been produced. The current *degree of corrosion* is the fraction of the maximum amount of gas produced at a certain time.

## 7.1 Water consumption

The COMP module offers three sources for water consumption:

1. the water contained in wastes and waste packages,

2. the water component of the liquid phase, and

3. the water implicitly contained in the brine component of the liquid phase.

The water mass contained in wastes and waste packages is input via parameter $m_{can}$. This water does not participate in the flow system. It is solely amenable to the corrosion process and consumed prior to the pore water.

Liquid consumption begins with the disappearance of canister water. The water component of the liquid is consumed first followed by the consumption of the brine component. The consumption rate for the brine component is higher than for the water com-

ponent since brine is not completely composed of water. Input parameter $r_{w/b}$ (COR-RO_waterMassPerBrineMass) determines the mass of water that is implicitly contained in a liquid with brine mass fraction 1.

Water consumption is enabled by setting CORRO_consumeWater to 1 and disabled by default. Canister water is always available for corrosion if water consumption has been enabled. Pore water consumption has to be enabled separately by setting parameter CORRO_consumePoreWater to 1. Pore water is unavailable for the corrosion process if liquid saturation falls below the saturation limit $S_{empty}^{CORRO}$ (CORRO_Sliqempty).

## 7.2 Gas component

The CORRO module requires the equation-of-state modules EOS7 and EOS7R and generates the non-condensible gas component of these EOS modules.

For reasons of simplicity we assume that gas is able to escape from the canister immediately, for example, because of pitting corrosion. The CORRO module therefore does not distinguish between gas produced inside and outside the waste canisters. The user should be aware that this assumption can be inadequate for some physical problems.

The main gas component of chemical iron corrosion is hydrogen but the non-condensable gas produced by EOS7 and EOS7R is air. If hydrogen should be the main gas component in the simulation, the properties of the gas component can be changed by means of the GCOMP module (see chapter 13).

Changing the gas component via GCOMP may be insufficient if the gas composition changes with time or location. The user should therefore reflect on possible errors resulting from the choice of a gas component that does not represent the gas component of the real system. Erroneous viscosity of the vapour-gas mixture causes errors in the gas flow. This should be corrected by choosing an appropriate viscosity function by means of the GCOMP module. A wrong atomic weight leads to errors in gas density as well as in the mass and mass fraction of the gas component. However, an erroneous atomic weight does not necessarily cause an erroneous transport of gas in terms of amount of substance. This has the following reasons.

- For a given amount of substance of a gas component, gas pressure is independent of atomic weight because of the implemented ideal gas law.

- Atomic weight has no major impact on liquid density if the mass fraction of dissolved gas is small (which usually is the case).

- According to Henry's law, the partial pressure of the main gas component is proportional to the mole fraction of the dissolved component. For this reason the amount of gas dissolved in liquid is independent of the gas component's atomic weight.

- The effect of the atomic weight on the diffusion of gas in the liquid phase is negligible. Let $\kappa$ be the gas component of TOUGH2-GRS and $\hat{\kappa}$ the real gas component. If the dissolved amount of gas is equal for both gas components (i. e. $n^\kappa = n^{\hat{\kappa}}$) and if we set the diffusion coefficient of component $\kappa$ equal to that of component $\hat{\kappa}$, i. e.

$$d^\kappa_\text{liq} := d^{\hat{\kappa}}_\text{liq},$$ 
(7.1)

  the diffusive flux of component $\kappa$ in the liquid phase is equal to that of the real component $\hat{\kappa}$ in terms of the amount of substance:

$$\frac{f^{\hat{\kappa}}_\text{liq}}{\mu_{\hat{\kappa}}} = \frac{f^\kappa_\text{liq}}{\mu_\kappa}$$ 
(7.2)

  with $f^\kappa_\beta$ being the diffusive mass flow in phase $\beta$ and $\mu_\kappa$ the atomic weight of component $\kappa$. Equation (7.2) is derived by substituting the diffusive mass flows with the corresponding TOUGH2 equation

$$f^\kappa_\beta = -\phi \tau_0 \tau_\beta \rho_\beta d^\kappa_\beta \nabla X^\kappa_\beta \,.$$ 
(7.3)

  This gives

$$m_\text{liq} d^\kappa_\text{liq} \nabla \frac{n^\kappa}{m_\text{liq}} = \widehat{m}_\text{liq} d^{\hat{\kappa}}_\text{liq} \nabla \frac{n^{\hat{\kappa}}}{\widehat{m}_\text{liq}}$$

  which again reduces to equation (7.1) under the approximation that dissolved gases only have little influence on liquid density and that liquid density is constant in space.

- The same operations applied to the diffusion in the gas phase lead to

$$m_\text{gas} d^\kappa_\text{gas} \nabla \frac{n^\kappa}{m_\text{gas}} = \widehat{m}_\text{gas} d^{\hat{\kappa}}_\text{gas} \nabla \frac{n^{\hat{\kappa}}}{\widehat{m}_\text{gas}} \,.$$ 
(7.4)

Gas masses $m_{\text{gas}}$ and $\hat{m}_{\text{gas}}$ depend on the atomic weights so that equation (7.3) reduces to

$$d^{\kappa}_{\text{gas}} = d^{\hat{\kappa}}_{\text{gas}} \tag{7.5}$$

only if either vapour or the main gas component is absent. Diffusion in the gas phase may therefore be affected by errors in atomic weight.

The user should therefore specify gas sources in terms of the amount of substance. The interpretation of the simulated gas transport should also focus on the amount of substance.

## 7.3        Gas generation rates

Each gas source is specified by the maximum amount of producible gas $N_{\text{tot}}$ (`COR-RO_moleGas`) and a gas generation rate $Q$. Corrosion experiments usually consider the rate of gas generation as a function of time $t$. We therefore use time-dependent rate functions to specify gas generation rates.

**Corrosion at full liquid saturation**

The CORRO module offers an exponential and a power law relationship to describe the corrosion rates for full liquid saturation (i. e. the entire gas source is in contact with water). The exponential function

$$Q_{\text{e}}(t) = A_{\text{liq}} e^{Bt} \quad , B < 0, \tag{7.6}$$

where $A_{\text{liq}}$ and $B$ are fitting parameters, is selected by `usePowerLaw=0`. The power law relationship

$$Q_{\text{p}}(t) = a \left( \frac{t - t_0}{t_{\text{ref}}} \right)^n \quad , n < 0 \quad \text{and} \quad t - t_0 \neq 0 \tag{7.7}$$

is selected by `usePowerLaw = 1`. Parameters $a$, $t_0$, $t_{\text{ref}}$, and $n$ are fitting parameters.

The amount of gas produced until time $t$ is

$$N(t) = \int_{\hat{t}=0}^{t} Q(\hat{t}) d\hat{t}. \tag{7.8}$$

Using equations (7.6) and (7.7) for $Q$ leads to

$$N(t) = \frac{A_{\text{liq}}}{B} (e^{Bt} - 1) \tag{7.9}$$

for the exponential function and

$$N(t) = \begin{cases} \dfrac{a\, t_{\text{ref}}}{n + 1} \left[ \left( \dfrac{t - t_0}{t_{\text{ref}}} \right)^{n+1} - \left( \dfrac{t_0}{t_{\text{ref}}} \right)^{n+1} \right] & \text{for} \quad n \neq -1 \\ a\, t_{\text{ref}} \ln \left( 1 + \dfrac{t}{t_0} \right) & \text{for} \quad = -1 \end{cases} \tag{7.10}$$

for the power law function.

Equations (7.6) and (7.7) are not implemented directly because time-discretization of production rates would lead to a rough approximation of the cumulative amount of produced gas according to equation (7.8). Instead, the mean production rate $\bar{Q}$ of time step $\Delta t$ is calculated by

$$\bar{Q}_{t_{\text{old}} \to t_{\text{old}}+\Delta t} := \frac{N(t_{\text{old}}+\Delta t) - N(t_{\text{old}})}{\Delta t}, \tag{7.11}$$

with starting time $t_{\text{old}}$ is. $\bar{Q}$ is the production rate under full liquid saturation. The production rate for limited water availability $\tilde{Q}$ will be derived from $\bar{Q}$ further below.

In order to calculate $\bar{Q}$ we need the amount of gas that had been produced at the last time step $N(t_{\text{old}})$. TOUGH2-GRS does not store $N(t_{\text{old}})$ but it stores the normalized value of $N(t_{\text{old}})$, which we call the *degree of corrosion*

$$g(t) := \begin{cases} \dfrac{N(t)}{N_{\text{tot}}} & \text{if less than 1} \\ 1 & \text{otherwise} \end{cases}. \tag{7.12}$$

$N_{\text{tot}}$ is the total amount of gas that can be produced by the source (an input parameter). Using the degree of corrosion, equation (7.11) can be rewritten as

$$\bar{Q}_{t_{\text{old}} \to t_{\text{old}}+\Delta t} := \frac{N(t_{\text{old}}+\Delta t) - g(t_{\text{old}}) N_{\text{tot}}}{\Delta t}. \tag{7.13}$$

**Corrosion with limited water availability**

Up to now, $Q$ and $N$ have been functions of time. To allow for a temporal stagnancy of corrosion, equation (7.13) is generalized by describing the time variable of rate function $Q$ as a function of the degree of corrosion

$$\theta: g \mapsto t \tag{7.14}$$

so that we receive

$$\bar{Q}_{t_{\text{old}} \to t_{\text{old}}+\Delta t} = \frac{N\big(\theta\big(g(t_{\text{old}})\big) + \Delta t\big) - g(t_{\text{old}}) N_{\text{tot}}}{\Delta t}. \tag{7.15}$$

The time function $\theta$ is derived by solving equation (7.12) with the help of equation (7.9) or (7.10), which gives us

$$\theta(g) = \frac{1}{B} \ln\left(\frac{gN_{\text{tot}}B}{A_{\text{liq}}} + 1\right) \tag{7.16}$$

for the exponential function and

$$\theta(g) = \begin{cases} \left[\dfrac{gN_{\text{tot}}(n+1)}{t_{\text{ref}}\, a} - \left(\dfrac{t_0}{t_{\text{ref}}}\right)^{n+1}\right]^{\frac{1}{n+1}} t_{\text{ref}} - t_0 & \text{for} \quad n \neq -1 \\ t_0\left(\exp\dfrac{gN_{\text{tot}}}{t_{\text{ref}}\, a} - 1\right) & \text{for} \quad = -1 \end{cases} \tag{7.17}$$

for the power law function.

Equations (7.16) and (7.17) are only used if `dependsOnTime=0`. Otherwise, the function $\theta(g) = t_{\text{old}}$ is used meaning that the corrosion rate decreases with time even if the corrosion process is stalled. The user should be aware that this usually is not a reasonable physical behaviour.

The production rate for limited water availability $\tilde{Q}$ is used as production rate for unlimited water supply $\bar{Q}$ unless water consumption is enabled (`CORRO_consumeWater=1`) and corrosion rates depend on the degree of corrosion (`corro_dependsOnTime=0`). In the following we consider the opposite case with $\tilde{Q} \neq \bar{Q}$.

If water consumption is enabled and corrosion rates depend on the degree of corrosion, the production rate for limited water availability $\tilde{Q}$ depends on how the switch `CORRO_AssumeWaterTable` is set. The switch decides which fraction of the gas source is in contact with water under unsaturated conditions. If the capillary fringe is small compared to the height of a grid element, we can assume the formation of a horizontal water table. Under these circumstances the element's liquid saturation can be viewed as the fraction $\alpha$ of the element that is below the water table, that is to say under full liquid saturation. Choosing `CORRO_AssumeWaterTable=1` sets $\alpha = S_{\text{liq}}$. In all other cases $\alpha$ is equal to 1.

If there is a water table, we define

$$\tilde{Q}_{t_{\text{old}} \to t_{\text{old}} + \Delta t} := \frac{\alpha A_{\text{liq}} e^{Bt} + (1 - \alpha) A_{\text{vap}}}{A_{\text{liq}}} \, \bar{Q}_{t_{\text{old}} \to t_{\text{old}} + \Delta t} \tag{7.18}$$

for the exponential function and

$$\tilde{Q}_{t_{\text{old}} \to t_{\text{old}} + \Delta t} := \alpha \, \bar{Q}_{t_{\text{old}} \to t_{\text{old}} + \Delta t} \tag{7.19}$$

for the power law function.


## 7.4　　Input data

Tab. 7.1 shows the input parameters of data block CORRO.

**Tab. 7.1**　Input format of data block CORRO

| Line | Column | Content | Format | Unit | Description | Variable |
|---|---|---|---|---|---|---|
| 1 | 1-5 | `"CORRO"` | A5 | | Keyword | |
| 2 | 1-10 | $R_{w/b}$ | G10.4 | – | Water mass per brine mass<br>Default: 0.46 | `CORRO_`<br>`waterMassPer-`<br>`BrineMass` |
| 2 | 11-20 | $S_{empty}^{CORRO}$ | G10.4 | – | Pore water consumption only if $S_{liq} > S_{empty}^{CORRO}$ | `CORRO_Sliqempty` |
| 3 | 1-5 | `"E","e",`<br>`"M","m"` | A5 | | Location type. Gas source is either placed in an element ("E", "e") or homogeneously distributed over a material ("M", "m"). | `CORRO_loctype(s)`<br><br>`s` is the source index |
| 3 | 6-10 | Location | A5 | | Element or material name | `CORRO_loc(s)` |
| 3 | 11-15 | Switch: consume water? | I5 | 1 | Stop gas generation in absence of water? 0: no, 1: yes | `CORRO_`<br>`consumeWater(s)` |
| 3 | 16-20 | Switch: consume pore water? | I5 | 1 | Stop gas generation in absence of pore water? 0: no, 1: yes | `CORRO_consume`<br>`PoreWater(s)` |
| 3 | 21-25 | Switch: Assume water table? | I5 | 1 | Recognize liquid saturation as relative height of a water table inside an element? 0: no, 1: yes | `CORRO_`<br>`assumeWater`<br>`Table(s)` |
| 3 | 26-30 | Switch: Use time-dependent rate function? | I5 | 1 | Calculate generation rates using the time instead of the degree of corrosion? 0: no, 1: yes | `CORRO_`<br>`dependsOnTime(s)` |
| 3 | 31-40 | $A_{liq}$ | G10.4 | mol/s | Fitting parameter of exponential rate function for water contact | `CORRO_Aliquid(s)` |
| 3 | 41-50 | $A_{vap}$ | G10.4 | mol/s | Fitting parameter of exponential rate function for vapour contact | `CORRO_Avapour(s)` |
| 3 | 51-60 | $B$ | G10.4 | 1/s | Fitting parameter of exponential rate function. 0: constant rate, <0: decreasing rate | `CORRO_B(s)` |
| 3 | 61-70 | – | – | – | INACTIVE | – |
| 3 | 71-80 | Switch: Use power function? | G10.4 | | Use power function instead of exponential function? 0: no, 1: yes | `CORRO_`<br>`useFunction2(s)` |
| 4 | 1-10 | $g_0$ | G10.4 | 1 | Initial degree of corrosion | `CORRO_`<br>`initialDegree`<br>`OfCorrosion(s)` |
| 4 | 11-20 | $N_{tot}$ | G10.4 | mol | Maximum amount of gas that can be produced | `CORRO_moleGas(s)` |
| 4 | 21-30 | $m_{can}$ | G10.4 | kg | Canister water | `CORRO_canister`<br>`WaterMass(s)` |
| 4 | 31-40 | $r_{w/g}$ | G10.4 | 1 | Mole of water consumed for every mole of gas that is produced | `CORRO_`<br>`moleWaterPer`<br>`MoleGas(s)` |
| 4 | 41-50 | $a$ | G10.4 | mol/s | Fitting parameter of power law rate function | `CORRO_f2_a(s)` |
| 4 | 51-60 | $n$ | G10.4 | 1 | Fitting parameter of power law rate function | `CORRO_f2_n(s)` |
| 4 | 61-70 | $t_0$ | G10.4 | s | Fitting parameter of power law rate function | `CORRO_f2_t0(s)` |
| 4 | 71-80 | $t_{ref}$ | G10.4 | s | Fitting parameter of power law rate function | `CORRO_f2_tref(s)` |
| *Repeat lines 3 and 4 for all gas sources* | | | | | | |

41

# 8 DEGRA: Time-dependent permeability changes

## 8.1 Model and implementation

The main function of technical seals is to prevent fluid flow. There are many physical and chemical processes contributing to seal degradation which is why a general-purpose module for the simulation of seal degradation must be very general and simple. Based on these considerations the DEGRA module introduces seal degradation as a time-dependent change of permeability. Intrinsic permeability is changed by means of a permeability modifier $f_{\mathrm{DEGRA}}$ (see chapter 2.7). Degradation takes place in a user-defined time window $[t_1, t_2]$ in which $f_{\mathrm{DEGRA}}$ increases linearly from 1 to the target value $F$:

$$
f_{\mathrm{DEGRA}} = \begin{cases} 1 & \text{for } t \le t_1 \\ 1 + \left(\dfrac{t - t_1}{t_2 - t_1}\right)(F - 1) & \text{for } t_1 < t < t_2 \\ F & \text{for } t \ge t_2 \end{cases} \tag{8.1}
$$

## 8.2 Input data

Tab. 8.1 shows the input data block of the DEGRA module.

**Tab. 8.1**     Input format of data block DEGRA

| Line | Column | Content | Format | Unit | Description | Variable |
|---|---|---|---|---|---|---|
| 1 | 1-5 | `"DEGRA"` | A5 | | Keyword | |
| 2 | 1-5 | material name | A5 | | Name of degrading material (as defined in ROCKS). In the following, `M` is the material index. | |
| 2 | 6-15 | $t_1$ | G10.4 | sec | Start time of permeability change $t_1$ | `DEGRA_T1(M)` |
| 2 | 16-25 | $t_2$ | G10.4 | sec | End time of permeability change $t_2$ | `DEGRA_T2(M)` |
| 2 | 26-35 | $F$ | G10.4 | 1 | Factor $F$ for the permeability at the time $t_2$ | `DEGRA_F(M)` |
| *Repeat line 2 for required materials* | | | | | | |

# 9 DOFT

DOFT is a new data block for domain-specific time series. It complements the existing data blocks FOFT, COFT, and GOFT, which are element-, connection-, and source-specific. Attention has to be paid with regard to the numbering of materials in the generated output file DOFT. Material 1 of the DOFT output file refers to entire model system excluding inactive elements. Since this domain is not (and cannot be) specified in the input data block, the first material of the DOFT input data block refers to the second material in the DOFT output file and so on. The content of the DOFT output file is described in chapter 0.

**Tab. 9.1** Input format of data block DOFT

| Line | Column | Content | Format | Unit | Variable |
|------|--------|---------|--------|------|----------|
| 1 | 1-5 | Keyword `"DOFT"` | A5 | | |
| 2 | 1-5 | Material | A5 | [1] | `edoft` |

*Repeat line 2 for all required materials. Material 1 will be the second material index in the DOFT file,*
*because the first index is reserved for the entire model domain.*

# 10 FISS: Gas pathway dilation

The transport of gas in low-permeability host rock, like clay stone or rock salt, becomes more efficient at high gas pressures. The increase of transport efficiency is not a gradual process but one that is controlled by pressure thresholds due to the opening of microscopic pathways, a process often referred to as "pathway dilation". At even higher pressures, macroscopic fracturing may take place.

The FISS module introduces several models for threshold-driven advective gas transport. Models for the change of pressure thresholds (softening), porosity, and gas permeability can be combined.

The FISS module makes use of the porosity change mechanism explained earlier in chapter 2.6. Changes of gas permeability do not affect intrinsic permeability but are introduced by adding a new permeability term to the flow equation for the gas phase. This is explained in chapter 10.3.

## 10.1 Pressure thresholds and softening models

We introduce a threshold pressure for the gas flow in dilating micro-fissures $p_{\text{thr}}$. The term softening will be used for a decrease of the threshold pressure. The decrease that takes place between successive time steps is denoted by $\Delta p_{\text{thr}}$ and it is controlled by a softening model that can be selected and specified by use of input parameters `ifsoft` and `fsoft` (see Tab. 10.1). The softening model `ifsoft` quantifies the change of threshold pressure $\widetilde{\Delta p}_{\text{thr}}$ required for an instantaneous equilibration of pressure and threshold pressure. Parameter `fsoft(3)` specifies how the value of $\widetilde{\Delta p}_{\text{thr}}$ is approached by the actual pressure change $\Delta p_{\text{thr}}$ with time.

**Equilibrium model**

- `ifsoft=0`: Constant threshold, no softening.

$$\widetilde{\Delta p}_{\text{thr}} = 0 \tag{10.1}$$

- `ifsoft=1`: Reversible linear softening.

The threshold pressure $p_{\mathrm{thr}}$ decreases linearly from $p_{\mathrm{thr,ini}}$ to $p_{\mathrm{thr,ini}} - \texttt{fsoft(2)}$ as $p$ increases from $p_{\mathrm{thr,ini}}$ to $p_{\mathrm{thr,ini}} + \texttt{fsoft(1)}$.

$$\widetilde{\Delta p}_{\mathrm{thr}} = \begin{cases} -p_{\mathrm{thr}} + p_{\mathrm{thr,ini}} & \text{for} & x_{\mathrm{thr}} < 0 \\ -p_{\mathrm{thr}} - x_{\mathrm{thr}} \cdot \texttt{fsoft(2)} + p_{\mathrm{thr,ini}} & \text{for} & 0 \le x_{\mathrm{thr}} \le 1 \\ -p_{\mathrm{thr}} - \texttt{fsoft(2)} + p_{\mathrm{thr,ini}} & \text{for} & x_{\mathrm{thr}} > 1 \end{cases} \tag{10.2}$$

with

$$x_{\mathrm{thr}} = \frac{p - p_{\mathrm{thr,ini}}}{\texttt{fsoft(1)}}. \tag{10.3}$$

- `ifsoft=2`: Irreversible linear softening. Same as `ifsoft=2` but positive values of $\widetilde{\Delta p}_{\mathrm{thr}}$ are clipped to zero.

**Time-dependency models**

- `fsoft(3)=0`: No time-dependency,

$$\Delta p_{\mathrm{thr}} = \widetilde{\Delta p}_{\mathrm{thr}}. \tag{10.4}$$

- `fsoft(3)=1`: Positive rate limit `fsoft(4)`,

$$\Delta p_{\mathrm{thr}} = \min\left(\left|\widetilde{\Delta p}_{\mathrm{thr}}\right|, \texttt{fsoft(4)}\,\Delta t\right)\, \mathrm{sgn}\left(\widetilde{\Delta p}_{\mathrm{thr}}\right). \tag{10.5}$$

- `fsoft(3)=2`: Rate decrease according to a decay function with half-life `fsoft(4)`,

$$\Delta p_{\mathrm{thr}} = \widetilde{\Delta p}_{\mathrm{thr}} \left(1 - 2^{-\frac{\Delta t}{\texttt{fsoft(4)}}}\right). \tag{10.6}$$

## 10.2 Fissure porosity models

Similar relations are used for fissure porosity. Parameter `ifpor` selects a model for the change of fissure porosity $\widetilde{\Delta \phi}_{\mathrm{fiss}}$ due to instantaneous equilibration. The actual change of fissure porosity $\Delta \phi_{\mathrm{fiss}}$ approaches $\widetilde{\Delta \phi}_{\mathrm{fiss}}$ according to time-dependency effects selected by parameter `fpor(matno,5)`.

**Equilibrium models**

- `ifpor=0`: No porosity change.

$$\widetilde{\Delta \phi}_{\mathrm{fiss}} = 0 \tag{10.7}$$

- `ifpor=1`: Porosity switches between two values. This model should only be used in combination with a kinetic model in order to avoid oscillations.

$$\widetilde{\Delta\phi}_{\text{fiss}} = \begin{cases} \texttt{fpor(1)} - \phi_{\text{fiss}} & \text{for} \quad p > p_{\text{thr}} \\ -\phi_{\text{fiss}} & \text{for} \quad p \leq p_{\text{thr}} \end{cases}. \tag{10.8}$$

- `ifpor=2`: Power-law behaviour with optional cut-off.

$$\widetilde{\Delta\phi}_{\text{fiss}} = \begin{cases} -\phi_{\text{fiss}} + \texttt{fpor(2)} & \text{for} \quad p > p_{\text{thr}} \wedge \texttt{fpor(4)} = 1 \\ -\phi_{\text{fiss}} + \texttt{fpor(2)}(x_{\text{por}})^{\texttt{fpor(3)}} & \text{for} \quad p > p_{\text{thr}} \wedge \texttt{fpor(4)} \neq 1, \\ -\phi_{\text{fiss}} & \text{for} \quad p \leq p_{\text{thr}} \end{cases} \tag{10.9}$$

with

$$x_{\text{por}} = \frac{p - p_{\text{thr}}}{\texttt{fpor(1)}}. \tag{10.10}$$

**Time-dependency models**

- `fpor(matno,5)=0`: No time-dependency.

$$\Delta\phi_{\text{fiss}} = \widetilde{\Delta\phi}_{\text{fiss}}. \tag{10.11}$$

- `fpor(matno,5)=1`: Positive rate limit `fpor(6)`.

$$\Delta\phi_{\text{fiss}} = \min\left(\left|\widetilde{\Delta\phi}_{\text{fiss}}\right|, \texttt{fpor(6)}\,\Delta t\right)\,\text{sgn}\left(\widetilde{\Delta\phi}_{\text{fiss}}\right). \tag{10.12}$$

- `fpor(matno,5)=2`: rate decrease according to an exponential decay function with half-life $b_6$.

$$\Delta\phi_{\text{fiss}} = \widetilde{\Delta\phi}_{\text{fiss}}\left(1 - 2^{-\frac{\Delta t}{\texttt{fpor(6)}}}\right). \tag{10.13}$$

## 10.3    Permeability models

The flow equation for the gas phase is extended by an additional term $k_{\text{dil}}\boldsymbol{K}_{\text{dil}}$ for the flow through fissures.

$$F_{\text{gas}} = -\frac{\rho_{\text{gas}}}{\mu_{\text{gas}}}\left(k\,k_{\text{r,gas}}\boldsymbol{I} + \underbrace{k_{\text{dil}}\boldsymbol{K}_{\text{dil}}}_{\substack{\text{micro crack}\\\text{permeability}}}\right)\left(\nabla p_{\text{gas}} - \rho_{\text{gas}}g\right) \tag{10.14}$$

$k$ is the intrinsic permeability, $k_{\mathrm{r,gas}}$ relative gas permeability, $\rho_{\mathrm{gas}}$ gas density, $\mu_{\mathrm{gas}}$ the dynamic viscosity of the gas phase, and $g$ the vector of gravitational acceleration. Variable $k_{\mathrm{dil}}$ is the pressure-dependent gas permeability of the fissure network, and tensor $\mathbf{K}_{\mathrm{dil},i}$ (input parameter `fiss_tensor`) introduces anisotropy.

It is assumed that micro cracks already opened by an intruding gas phase remain unsaturated, and for this reason no relative gas permeability is introduced for the micro crack network.

The two terms in the large brackets of equation (10.14) stand for the permeability of the original pore space and that of the secondary pore space created by pathway dilation. In the space-discretised version of equation (10.14), these two terms are weighted separately with $k_{\mathrm{dil}}\boldsymbol{K}_{\mathrm{dil}}$ always being upstream-weighted.

$k_{\mathrm{dil}}$ is defined as a power function with lower and optional upper cut-off

$$
k_{\mathrm{dil}}
= \begin{cases}
\texttt{fper(3)} & y < 0 \\
\texttt{fper(4)} & y > 1 \wedge \texttt{fper(6)} \neq 0 \\
y^{\texttt{fper(5)}} \cdot (\texttt{fper(4)} - \texttt{fper(3)}) + \texttt{fper(3)} & \text{otherwise}
\end{cases} \tag{10.15}
$$

with

$$
y = \frac{x - \texttt{fper(1)}}{\texttt{fper(2)} - \texttt{fper(1)}}. \tag{10.16}
$$

Parameter `fper(6)` introduces an upper cutoff of $k_{\mathrm{dil}}$. The meaning of $x$, `fper(1)`, and `fper(2)` depends on the choice of `ifper`:

- `ifper=0`: $x = $ `fper(1)` (constant permeability $k_{\mathrm{dil}} = $ `fper(3)`)

- `ifper=1`: $x = \phi_{\mathrm{fiss}}$ ($k_{\mathrm{dil}}$ is a function of fissure porosity)

- `ifper=2`: $x = p - p_{\mathrm{thr}}$ ($k_{\mathrm{dil}}$ is a function of gas pressure)

- `ifper=3`: $x = p_{\mathrm{thr}}$ ($k_{\mathrm{dil}}$ is a function of the pressure threshold)

## 10.4　　　　Input data

Tab. 6.1 shows the parameters of input data block FISS. Micro-fissuring is activated for materials.

**Tab. 10.1**　Input format of data block FISS

| Line | Column | Content | Format | Unit | Description | Variable |
|------|--------|---------|--------|------|-------------|----------|
| 1 | 1-5 | `"FISS"` | A5 | | Keyword | |
| 2 | 1-5 | Material name | A5 | | Name of compacting material (as defined in ROCKS)<br>In the following, `M` is the material index. | |
| 3 | 1-10 | $p_{\mathrm{thr,ini}}$ | G10.4 | Pa | Initial pressure threshold | `ptini(M)` |
| 4 | 1-5 | | I5 | | Softening model | `ifsoft(M)` |
| | 11-20 | | G10.4 | | Parameter 1 of softening model | `fsoft(M,1)` |
| | | | | | … | |
| | 71-80 | | G10.4 | | Parameter 7 of softening model | `fsoft(M,7)` |
| 5 | 1-5 | | I5 | | Porosity model | `ifpor(M)` |
| | 11-20 | | G10.4 | | Parameter 1 of porosity model | `fpor(M,1)` |
| | | | | | … | |
| | 71-80 | | G10.4 | | Parameter 7 of porosity model | `fpor(M,7)` |
| 6 | 1-5 | | I5 | | Permeability model | `ifper(M)` |
| | 11-20 | | G10.4 | | Parameter 1 of permeability model | `fper(M,1)` |
| | | | | | … | |
| | 71-80 | | G10.4 | | Parameter 7 of permeability model | `fper(M,7)` |
| 7 | 31-40 | | G10.4 | [1] | Permeability factor for ISO=1 | `fiss_tensor(M,1)` |
| | 31-40 | | G10.4 | [1] | Permeability factor for ISO=2 | `fiss_tensor(M,2)` |
| | 31-40 | | G10.4 | [1] | Permeability factor for ISO=3 | `fiss_tensor(M,3)` |
| *Repeat line 2 to 7 for all dilating materials* | | | | | | |

# 11 GCOMP: Primary non-condensable gas component

Air is the primary non-condensable gas component of EOS7 and EOS7R, which usually is an appropriate choice for the time immediately after repository closure. Due to gas-producing processes, other gas components may evolve and become predominant. Module GCOMP allows to change characteristics of the primary non-condensable gas component in terms of absolute molecular weight $M_{gas}$, specific enthalpy $h_{gas}$, inverse Henry constant $H_{inv}$ , and viscosity of the gas-vapour mixture.

## 11.1 Absolute molecular weight

The absolute molecular weight of the non-condensable gas can be changed by input parameter $M_{ncg}$ (GCOMP_AM), which has to be defined in units of kg/mol (note that the absolute molecular weight variables AMA of EOS7 and EOS7R are defined in units of g/mol). Because the composition of the main gas component can change with time and place, $M_{ncg}$ might not be the correct molecular weight for the entire simulation. However, many processes are not sensitive to errors in molecular weight if the amount of substance is correct. This applies to

- partial pressures (because EOS7 and EOS7R assume ideal gasses),

- the Henry law (which only depends on the amount of substance),

- advective flow of the gas component (because the mass of dissolved gas usually is too small to influence fluid density), and

- diffusive flow of the gas component in the liquid phase (which only depends on the amount of substance).

Simulations may therefore use erroneous molecular weights of the primary non-condensable gas component. These errors affect component masses but not their amount of substance.

## 11.2 Specific enthalpy

By setting $h_{gas} > 0$ (GCOMP_CV), the specific enthalpy of the main non-condensable gas component is set to $h_{gas}$. In case of $h_{gas} \leq 0$, the default value of the respective EOS

module is used, which is 733 J/mol for EOS7 and EOS7R (air), and 10,170 J/mol for EOS5 (hydrogen).

## 11.3 Inverse Henry constant

The temperature-dependency of the inverse Henry is calculated using a cubic polynomial with lower cut-off $H_{\text{inv,min}}$

$$H_{\text{inv}} = \max\left(H_{\text{inv,min}}, a_1 + a_2\vartheta + a_3\vartheta^2\right), \tag{11.1}$$

where $\vartheta$ is the temperature in degree Celsius. The equation is only applied if $H_{\text{inv}} \neq 0$. Otherwise, GCOMP uses the inverse Henry constant of the EOS module.

## 11.4 Gas phase viscosity

The GCOMP module offers three viscosity functions for vapour-bearing gases:

- **Hydrogen only (no vapour)**

  GCOMP_VISFUN = "H2" selects the viscosity function of the EOS5 module.

- **Air and vapour**

  GCOMP_VISFUN = "Air-H2O" selects the viscosity function of the EOS7 and EOS7R module.

- **Hydrogen and vapour**

  This viscosity function is selected by GCOMP_VISFUN = "H2-H2O".

Viscosity function 3 is based on the temperature-dependent viscosity function of /LAN 69/ for a $H_2$-vapour mixture, which we have extended by a pressure-dependent correction factor $h(p)$:

$$\eta_{H_2}\left(T, p, x_{H_2}\right) = f(T) \cdot g\left(x_{H_2}\right) \cdot h(p) \cdot 191.8 \cdot 10^{-7}\,\text{Pa s.} \tag{11.2}$$

$T$ is the temperature in Kelvin, $p$ is the gas pressure, and $x_{H_2}$ the mass fraction of $H_2$. The function $f(T)$ is given by

$$f(T) = \left(\frac{T}{273.16 \text{ K}}\right)^n \tag{11.3}$$

with

$$n = x_{H_2}\left(0.674 - 0.034 \cdot 10^{-4}\frac{\vartheta}{1\,°C}\right) + x_{H_2O}\left(1.082 - 0.25 \cdot 10^{-4}\frac{\vartheta}{1\,°C}\right). \tag{11.4}$$

Function $g(x_{H_2})$ is defined by

$$g(x_{H_2}, x_{H_2O}) =$$
$$\left(1 + \sqrt{2\left(2.016\, x_{H_2} + 18.016\, x_{H_2O}\right)}\right) \frac{0.6355\, x_{H_2} + 0.439\, x_{H_2O}}{4.36\, x_{H_2} + 6.31\, x_{H_2O}} \tag{11.5}$$

with $x_{H_2O} = 1 - x_{H_2}$.

The pressure-dependency of the viscosity

$$h(p) = \left(\frac{p}{101325 \text{ Pa}}\right)^{0.005} \tag{11.6}$$

has been derived from the relation that is implemented in the viscosity routine of EOS5 for pure hydrogen. It has to be regarded as an approximation.

## 11.5 Input data

The input parameters of module GCOMP are summarized in Tab. 11.1.

**Tab. 11.1**  Input format of data block GCOMP

| Line | Column | Vontent | Format | Unit | Description | Variable |
|------|--------|---------|--------|------|-------------|----------|
| 1 | 1-5 | `"GCOMP"` | A5 | | Keyword | |
| 2 | 1-10 | $M_{ncg}$ | G10.4 | kg/mol | Absolute molecular weight | GCOMP_AM |
| 2 | 11-20 | $h_{gas}$ | G10.4 | J/mol | Specific enthalpy | GCOMP_CV |
| 2 | 21-30 | $a_1$ | G10.4 | $Pa^{-1}$ | Coefficient 1 for the calculation of the inverse Henry constant | GCOMP_HC1 |
| 2 | 31-40 | $a_2$ | G10.4 | $Pa^{-1}$ $°C^{-1}$ | Coefficient 2 for the calculation of the inverse Henry constant | GCOMP_HC2 |
| 2 | 41-50 | $a_3$ | G10.4 | $Pa^{-1}$ $°C^{-2}$ | Coefficient 3 for the calculation of the inverse Henry constant | GCOMP_HC3 |
| 2 | 51-60 | $H_{inv,min}$ | G10.4 | $Pa^{-1}$ | Minimum value for the inverse Henry constant | GCOMP_HCMIN |
| 2 | 61-70 | `"Air-H2O"`, `"H2-H2O"` or `"H2"` | A10 | | Viscosity function selector | GCOMP_VISFUN |

## 12 PRLIM: Gas pressure limitation

### 12.1 Model and implementation

Modelling grids for repositories in rock salt usually do not include the impermeable host rock. However, it may happen that the host rock becomes permeable to gas flow if gas pressures approach the minimal principal stress by the opening of fissures or fractures. The escape of gas from the repository into the host rock can be modelled even if the host rock is not part of the modelling grid. For this purpose, module PRLIM clips the gas pressures inside the model to the desired threshold pressure. The accumulated loss of gas due to the clipping is printed.

Microscopic pathway can already open below the minimal principal stress due to microscopic heterogeneities of the material and stress field. The entry pressure is therefore defined relative to the minimal principal stress by means of a pressure offset $\Delta_{\text{dilat}}$:

$$p_{\text{entry}} = \sigma_{\min} - \Delta_{\text{dilat}}. \tag{12.1}$$

Module PRLIM allows to define parameter $\Delta_{\text{dilat}}$ separately for every material. Module PRLIM introduces minimal principal stress $\sigma_{\min}$ as a linear function of depth $z$

$$\sigma_{\min}(z) = \sigma_{\min,\text{ref}} + (z - z_{\text{ref}}) \frac{\mathrm{d}\sigma_{\min}}{\mathrm{d}z}. \tag{12.2}$$

Parameter $\sigma_{\min,\text{ref}}$ is the minimal principal stress at reference depth $z_{\text{ref}}$ and the factor $\mathrm{d}\sigma_{\min}/\mathrm{d}z > 0$ is the vertical gradient of the minimal principal stress. We neglect that stresses can change in the vicinity of mining cavities.

## 12.2 Input data

Tab. 12.1 shows the input data block of module PRLIM.

**Tab. 12.1**  Input format of data block PRLIM

| Line | Column | Content | Format | Unit | Description | Variable |
|------|--------|---------|--------|------|-------------|----------|
| 1 | 1-5 | "PRLIM" | A5 | | Keyword | |
| 2 | 1-10 | $z_{\mathrm{ref}}$ | G10.4 | m | | PRLIM_ZREF |
| 2 | 11-20 | $\sigma_{\mathrm{min,\,ref}}$ | G10.4 | Pa | | PRLIM_P |
| 2 | 21-30 | $\dfrac{d\sigma_{\mathrm{min}}}{dz}$ | G10.4 | Pa/m | | PRLIM_DPDZ |
| 3 | 1-5 | Material name | A5 | | Activate PRLIM for this material. M ist he material index in the following | |
| 3 | 6-15 | $\Delta_{\mathrm{dilat}}$ | G10.4 | Pa | $\Delta_{\mathrm{dilat}}$ | PRLIM_POFFSET(M) |
| *Repeat line 3 for all materials that introduce pressure limitation* | | | | | | |

# 13　PTIME: High-precision printout times

Module PTIME works in the same way as data block TIMES except for the higher pre-cision of time values and the extension to 10,000 time entries. If data block PTIME is present, it overwrites the TIMES block. Tab. 13.1 shows the structure of the PTIME data block, which resembles data block TIMES.

**Tab. 13.1**　Input format of data block PTIME

| Line | Column | Content | Format | Unit | Description | Variable |
|------|--------|---------|--------|------|-------------|----------|
| 1 | 1-5 | `"PTIME"` | A5 | | Keyword | |
| 2 | 1-5 | Number of times in table | I5 | 1 | Must not be larger than 100 | ITI |
| 2 | 6-10 | Number of times to be used | I5 | 1 | Must be larger or equal to ITI. If larger than ITI, printout times will be distributed according to TINTER. | ITE |
| 2 | 11-20 | Maximum time step | G10.4 | s | Upper limit for the time step size after first printout time. Inactive if zero. | DELAF |
| 2 | 21-30 | Time incre-ment for printouts ITI to ITE | G10.4 | s | Only active if ITE > ITI | TINTER |
| ≥3 | 1-20, 21-40, 41-60, 61-80 | Table of printout times (ascending order) | 4G20.14 | s | | TIS(I) |

# 14 RANGE: Limiting primary variables

Transitions between one-phase states and two-phase states can be numerically problematic causing bad convergence and a drastic reduction of time step size. A possible workaround is to keep the system in a two-phase state by restricting gas saturation to values above 0 and below 1.

Another numerical problem is that brine mass fraction can run out of bounds if water saturation is very low. The reason is that erroneous brine mass fractions do not violate the absolute convergence criterion if liquid saturation is very small. Brine mass fractions beyond physical meaning need not be a numerical problem but they hinder a meaningful visualisation of the brine mass fraction. One might therefore want to clip the brine mass fraction to reasonable values.

The RANGE module allows to restrict the range of both, gas saturation and brine mass fraction. This can involve a clipping of primary variables that violates mass conservation. The physical system parameter should therefore be chosen such that clipping is avoided as far as possible.

## 14.1 Limiting brine mass fraction

Brines are defined by the equation-of-state modules EOS7 and EOS7R as mixture of pure water and a reference brine. The mass ratio between the reference brine and the liquid is the brine mass fraction. Following this concept, the brine mass fraction cannot be larger than 1 without sacrificing the idea of mixing two liquids. However, if the specified reference brine is regarded as an intermediate mixing product, brine mass fractions beyond 1 can be physically plausible and TOUGH2 does not object to such values.

Errors in the estimation of the brine mass fraction do not necessarily lead to a violation of convergence criteria because the convergence criteria evaluate mass conservation, not mass fraction conservation. If liquid saturation is low, the absolute errors of brine mass are small too. TOUGH2 therefore tolerates large errors in brine mass fraction if grid elements are almost dry. In turn, the estimated brine mass fraction may exceed the value of 1 by far. This is not a problem in terms of mass conservation but may contra-

dict the idea of mixing two types of liquid. Grid elements with very high brine mass fractions also complicate the visual interpretation of the simulation output.

By setting `RANGE_restrictXb = 1`, the brine mass fraction is restricted to the interval [`RANGE_XBmin`, `RANGE_XBmax`]. This is achieved by clipping the values of the corresponding primary variable. For the reasons mentioned above, this should not significantly violate mass conservation. Setting `RANGE_XBmin = 0` and `RANGE_XBmax = 1` should be appropriate in many cases unless other process modules like CORFL require brine mass fractions above 1.

## 14.2 Constant brine mass fraction

Setting `RANGE_equilibrateXb = 1` keeps the brine mass fraction at a constant value `RANGE_EQ_Xbr`. The intention may be to simulate a chemical equilibrium of the solution with salt rock, which would result in a constant brine mass fraction.

If the RANGE modules keeps the brine mass fraction constant it conserves the total water mass. This includes the water implicitly contained in the reference brine. The ratio between brine mass and contained water mass is passed by parameter `RANGE_EQ_BrineMassPerWaterMass`.

Keeping the brine mass fraction constant is incompatible with the CORFL module, because this module uses the brine mass fraction as a marker for the fluid's corrosion capability. The interference with the CORRO module is not well tested.

## 14.3 Clipping gas saturation and reducing vapour pressure

Setting `RANGE_restrictSg` = 1 restricts *gas saturation* (a primary variable) to the interval `RANGE_SGmin` to `RANGE_SGmax`. Choosing `RANGE_SGmin` >0 and `RANGE_SGmax` < 1 preserves a two-phase state. The clipping operation involved violates mass conservation and should therefore be avoided as much as possible. The system should be designed to remain in a two-phase state by itself, for example by introducing residual saturations to the relative permeability function. Further on, capillary pressures may prevent desaturation of elements. Yet, the disappearance of a phase cannot be entirely prevented by these measures for the following reasons:

- Even an immobile gas phase can be displaced by way of gas dissolution and advective transport of dissolved gas in the liquid phase.

- Even an immobile liquid phase can be displaced by evaporation and advective transport of vapour in the gas phase.

- Backfill compaction, induced by the COMP module, compresses the gas phase thereby increasing gas dissolution. If the liquid saturation is near to one the gas phase can disappear.

To prevent evaporation of the entire liquid phase, the RANGE module also offers to reduce the saturation vapour pressure. By setting `RANGE_reducePs = 1` the vapour pressure decreases linearly to zero as gas saturation increases from `RANGE_PS_SGmin` to `RANGE_PS_SGmax`. The user should set `RANGE_PS_SGmax < RANGE_SGmax` to prevent the RANGE module from clipping the gas saturation (see Fig. 14.1).
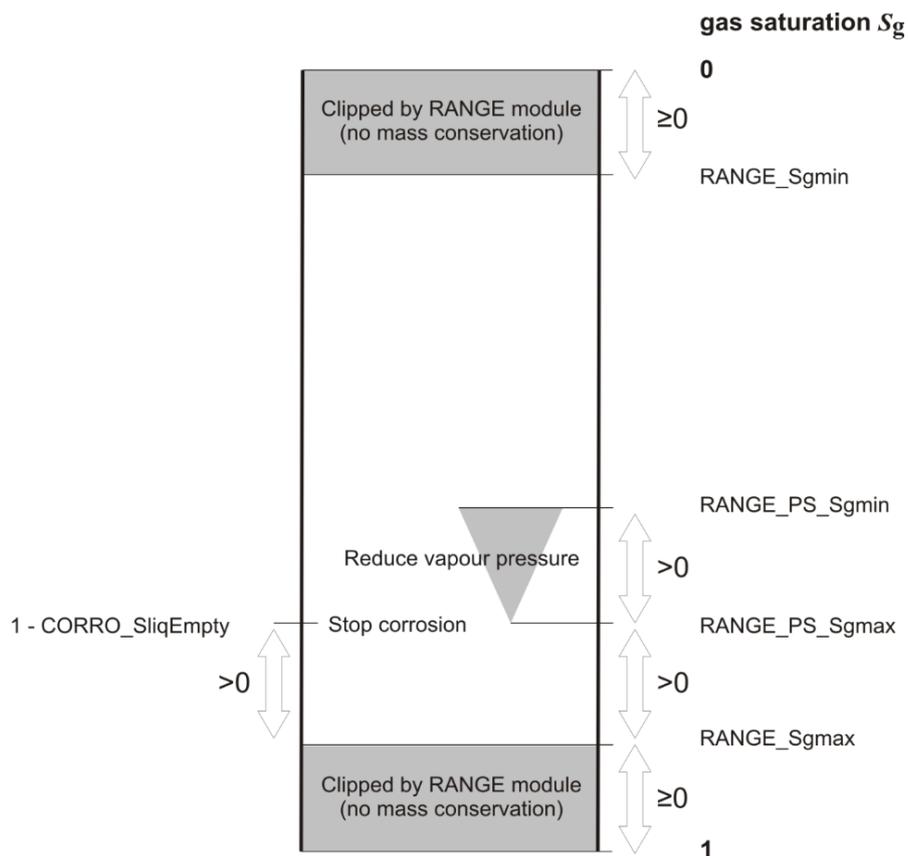


**Fig. 14.1** Relationship between saturation limits of the RANGE and CORRO modules

## 14.4 Input data

The input parameters of module RANGE are listed in Tab. 14.1.

**Tab. 14.1** Input format of data block RANGE

| Line | Column | Content | Format | Unit | Variables |
|------|--------|---------|--------|------|-----------|
| 1 | 1-5 | Keyword `"RANGE"` | A5 | | |
| 2 | 1-10 | **Limit brine mass fraction?** <br> 0: No. <br> 1: Yes. Restrict to interval $[X_{b,min}, X_{b,max}]$. | G10.4 | 1 | `RANGE_restrictXb` |
| 2 | 11-20 | Lower limit of the brine mass fraction | G10.4 | 1 | `RANGE_XBmin` |
| 2 | 21-30 | Upper limit of the brine mass fraction | G10.4 | 1 | `RANGE_XBmax` |
| 3 | 1-10 | **Constant brine mass fraction?** <br> 0: No <br> 1: Yes. | G10.4 | 1 | `RANGE_equilibrateXb` |
| 3 | 11-20 | Brine mass fraction in equilibrium. | G10.4 | 1 | `RANGE_EQ_Xbr` |
| 3 | 21-30 | Brine mass per mass of contained water. | G10.4 | 1 | `RANGE_EQ_BrineMassPerWaterMass` |
| 4 | 1-10 | **Limit gas saturation?** <br> 0: No. <br> 1: Yes. | G10.4 | 1 | `RANGE_restrictSg` |
| 4 | 11-20 | Lower limit of gas saturation | G10.4 | 1 | `RANGE_SGmin` |
| 4 | 21-30 | Upper limit of gas saturation (has to be larger than the lower limit) | G10.4 | 1 | `RANGE_SGmax` |
| 5 | 1-10 | **Dim saturation vapour pressure?** <br> 0: No. <br> 1: Yes. Reduce saturation vapour pressure linearly as gas saturation rises from $S_{g,dim}$ to $S_{g,zero}$. <br><br> $S_{g,dim} < S_{g,zero} \leq 1$ | G10.4 | 1 | `RANGE_reducePs` |
| 5 | 11-20 | $S_{g,dim}$ | G10.4 | 1 | `RANGE_PS_SGmin` |
| 5 | 21-30 | $S_{g,zero}$ | G10.4 | 1 | `RANGE_PS_SGmax` |

# 15 RELA: permeability and capillary pressure functions

The RELA module introduces functional dependencies for permeability and capillary pressure. For reasons of downward compatibility, these functions are also part of the COMP module. However, the user is advised to use the corresponding features of the RELA module, which override those of the COMP module.

## 15.1 Porosity-permeability relationships

Experimental studies with compacting salt grit have shown power law relationships between permeability and porosity for certain porosity ranges /KRÖ 09/. The COMP module introduces piecewise-defined porosity-permeability relationships with up to five power subfunctions

$$k = a_i \, \phi^{b_i} \tag{15.1}$$

with $k$ being the (isotropic) intrinsic permeability and $\phi$ the porosity. Parameters $a_i$ and $b_i$ ($1 \leq i \leq 5$) are fitting parameters.

The porosity domain of each subfunction is determined by the intersections of adjacent subfunctions $i$ and $i + 1$. Subfunctions must be defined in the order of descending porosity in input data block COMP meaning that subfunction $i$ refers to higher porosities than subfunction $j > i$.

Permeability is set to zero if the lower porosity limit $\phi_{k=0}$ is set to a positive value

$$k = 0 \quad \text{for} \quad \phi \leq \phi_{k=0} \,. \tag{15.2}$$

Note that only isotropic permeabilities are available.

## 15.2 Change of capillary pressures

Backfill compaction affects capillary pressures by changing the backfill's pore structure. The COMP module allows to approximate this effect by means of the Leverett's J-function /LEV 41/

$$p_{\mathrm{c}}(S) = p_{\mathrm{c}0}(S) \left( \frac{k_0 \phi}{\phi_0 k} \right)^{\alpha}. \tag{15.3}$$

$p_{\mathrm{c}}$ is the capillary pressure at liquid saturation $S$, porosity $\phi$, and permeability $k$. Function $p_{\mathrm{c}0}(S)$ is the unscaled capillary pressure function of the initial porosity $\phi_0$ and permeability $k_0$ as defined by data block ROCKS. If the user chooses $p_{\mathrm{c}0}$ to be the van Genuchten function (`ICP = 7`), the maximum capillary pressure cut-off `CP(4)` is applied to the scaled function, too.

## 15.3      Temperature-dependent capillary pressures

According to /GRA 14/, capillary pressure decreases with temperature, and capillary pressure functions for different temperatures relate to each other by

$$p_{\mathrm{c}}(S, T) = p_{\mathrm{c}}(S, T_{\mathrm{ref}}) \frac{\beta + (T + 273.15)}{\beta + (T_{\mathrm{ref}} + 273.15)}, \tag{15.4}$$

where $T$ is the temperature in °C and $p_{\mathrm{c}}(S, T_{\mathrm{ref}})$ the capillary pressure function at temperature $T_{\mathrm{ref}}$ (also in °C). Constant $\beta$ is defined by

$$\beta := \frac{a}{b} \tag{15.5}$$

with $a$ and $b$ being constants of the dependency of the liquid-gas interface tension on temperature

$$\gamma^{\mathrm{lg}} = a + b \, (T + 273.15) \tag{15.6}$$

According to /GRA 14/, $\beta$ varies between -800 K and -330 K and values of -566 K and 438 K have been found for silt loam. Both input parameters of the RELA data block, $\beta$ and $T_{\mathrm{ref}}$, are input in degrees Celsius.

## 15.4      Input data

The input data of module RELA are listed in Tab. 15.1.

**Tab. 15.1**  Input format of data block RELA

| Line | Column | Content | Format | Unit | Description | Variable |
|---|---|---|---|---|---|---|
| 1 | 1-5 | "RELA" | A5 | | Keyword | |
| 2 | 1-5 | Material name | A5 | | Name of compacting material (see card ROCKS). M is the material index. | |
| 3 | 1-10 | $K_{\text{ref}}$ | G10.4 | [sec$^{-1}$] | Reference convergence rate | COMP_KREF(M) |
| | 11-20 | $f_{\text{loc}}$ | G10.4 | [1] | Local modification of the reference convergence rate | COMP_FLOC(M) |
| | 21-30 | $p_G$ | G10.4 | [Pa] | Lithostatic pressure at the location if no cavity would exist | COMP_PG(M) |
| | 31-40 | $m_p = m_\phi$ | G10.4 | [1] | Exponent for the calculation of $f_p$ | COMP_M(M) |
| | 41-50 | $\phi_r$ | G10.4 | [1] | Porosity at which backfill support commences | COMP_PHIref(M) |
| | 51-60 | $h_1$ | G10.4 | [1] | Parameter for the calculation of $f_\phi$ | COMP_H1(M) |
| | 61-70 | $g_1$ | G10.4 | [1] | Parameter for the calculation of $f_\phi$ | COMP_G1(M) |
| | 71-80 | $g_2$ | G10.4 | [1] | Parameter for the calculation of $f_\phi$ | COMP_G2(M) |
| 4 | 1-10 | $\lambda_s$ | G10.4 | [1] | Parameter for the calculation of $f_T$ | COMP_LAMBDAS(M) |
| | 11-20 | $K_0$ | G10.4 | [sec$^{-1}$] | Initial convergence rate | COMP_K0(M) |
| | 21-30 | $a$ | G10.4 | [1] | Weighting factor for creep processes | COMP_A(M) |
| | 31-40 | $Q_1$ | G10.4 | [J/mol] | Activation energy for creep process 1 | COMP_Q1(M) |
| | 41-50 | $Q_2$ | G10.4 | [J/mol] | Activation energy for creep process 2 | COMP_Q2(M) |
| | 51-60 | $T_{\text{ref}}$ | G10.4 | [°C] | Temperature of the rock at the reference location | COMP_TGREF(M) |
| | 61-70 | $\phi_{\text{lim}}$ | G10.4 | [1] | Lower porosity limit for the convergence process (may be 0) | COMP_PHIMIN(M) |
| 5 | 1-10 | 0 or 1 | I10 | [1] | Enable Leverett scaling of capillary pressures? (0 = no, 1 = yes) | COMP_LEVQ(M) |
| | 11-20 | $k_0$ | G10.4 | [m²] | Reference permeability for Leverett scaling | COMP_LEVPERREF(M) |
| | 21-30 | $\phi_0$ | G10.4 | [1] | Reference porosity for Leverett scaling | COMP_LEVPHIREF(M) |
| | 31-40 | $\alpha$ | G10.4 | [1] | Exponent of the Leverett scaling | COMP_LEVEXP(M) |
| 6 | 1-10 | $\phi_{k=0}$ | G10.4 | [1] | Permeability will be 0 for porosities $\leq \phi_{k=0}$ | COMP_CUTOFF(M) |
| 7 | 1-10 | $n_{\text{sec}}$ | I10 | [1] | Number of subsections of the porosity-permeability relation | COMP_NBRANCH(M) |
| 8 | 1-10 | $a_i$ | G10.4 | [m²] | Factor of power law $i$ | COMP_PERA(I,M) |
| | 11-20 | $b_i$ | G10.4 | [m²] | Exponent of power law $i$ | COMP_PERB(I,M) |
| *Repeat line 8 for all $n_{\text{sec}}$ sections* | | | | | | |
| last | 1-10 | 0 or 1 | I10 | 1 | Enable temperature-dependent capillary pressures? (0 = no, 1 = yes) | COMP_LEVQ(M) |
| | 11-20 | $\beta$ | G10.4 | °C | | rela_PCTBETA (M) |
| | 21-30 | $T_{\text{ref}}$ | G10.4 | °C | | rela_PCTTREF (M) |
| *Repeat from line 2 for all materials concerned* | | | | | | |

# 16          RN

Module RN simulates decay, transport, sorption and anion exclusion of radionuclide chains of arbitrary size. It operates on top of the TOUGH2 flow simulation without affecting them. The module can therefore be used with every EOS module.

## 16.1          Links to standard TOUGH2

The RN module calculates the decay of radionuclides first. In every time step of the ensuing transport calculation, the phase distribution of radionuclides is determined as well as the advective and diffusive radionuclide fluxes.

The transport equations were taken from the TOUGH2 core to achieve the same transport behavior. The equations describing the phase distribution of radionuclides are derived from the equations of the EOS7R module but also include linear sorption.

Required transport parameters like, for instance, weighting parameters, are obtained from the regular TOUGH2 input. However, there is a little difference regarding the `NB` parameter of block MULTI because diffusive transport of radionuclides is also possible if no diffusion (`NB`=6) is selected in MULTI.

Please note that the radionuclide masses placed in the system with the RN module are *total* masses. They are composed of the masses in all phases (solid, liquid, and gas). On the contrary, radionuclide masses placed in a two-phase state in connection with the EOS7R module are dissolved masses *after the distribution process* and do not include adsorbed masses or masses in the gas phase.

## 16.2          Time stepping and performance

The RN module uses a time integration algorithm that implements the Bulirsch-Stoer method /STO 80/. Owing to this new solver there are now three steps of time discretization:

1. Time discretization by the CYCIT routine of TOUGH2 yielding time step size $\Delta t_{T2}$ (which is the standard time step size `DELTEX` of TOUGH2).

2. The subdivision of $\Delta t_{t2}$ by the time stepping routine of the Bulirsch-Stoer solver yielding the time step size $\Delta t_{BS}$.

3. The successive subdivision of $\Delta t_{BS}$ in 2, 4, 6, 8, 10, 12, 14, 16, and 18 equal parts used for the extrapolation part of the Bulirsch-Stoer method. The successive division of $\Delta t_{BS}$ is stopped as soon as convergence is achieved. We use $n_{ex}$ to refer to the number of subdivisions made.

Convergence is tested in step 3. If convergence is not achieved, three things can happen:

- Time step $\Delta t_{BS}$ is further subdivided ($n_{ex}$ is increased)

- Time step $\Delta t_{BS}$ is reduced

- Time step $\Delta t_{T2}$ is reduced

For some problems, the performance of the simulation heavily depends on how these measures are balanced. To achieve good performance, the numerical effort that has been made before a time step is discarded should be as low as possible. Particularly, it has to be decided whether a reduction of $\Delta t_{BS}$ is a better choice that an increase of $n_{ex}$. Although increasing $n_{ex}$ improves the quality of extrapolation it is connected with a non-linear increase of calculation time, partly due to the mounting inter-process communication of TOUGH2-MP-GRS. Reduction of $\Delta t_{BS}$ appears to be a better choice if convergence by subdivision of $\Delta t_{BS}$ is not achieved quickly. We therefore stop increasing $n_{ex}$ and reduce $\Delta t_{BS}$ instead, if the errors for each $n_{ex}$ do not decrease by a factor of $f_{ex}$. For some problems, $f_{ex} = 0.6$ has yielded a speed increase by a factor of about 10.

Radionuclides that are very mobile should be defined first in data block RN. The reason is that TOUGH2-GRS and TOUGH2-MP-GRS handle radionuclides in the succession of their definition and that mobile radionuclides are the ones that most likely introduce convergence problems. Defining them first spares transport calculations for the less problematic radionuclides.

The RN module is the only process module that simulates fluxes between elements. For this reason, its overhead due to inter-process communication is considerably higher than for other process modules (so called "external elements" have to be exchanged). If many radionuclides are present the serial code TOUGH2-GRS can show a better performance than the multi-processor code TOUGH2-MP-GRS.

## 16.3    Simulation controls

Parameters controlling accuracy and performance are conveyed by the first line of data block RN. These are, in order of definition:

- Relative tolerance (default: 1E-7)
- Absolute tolerance in kg (default: 1E-30 kg)
- Maximum steps of the Burlirsch-Stoer stepper (default: 1000)
- Choice of the extrapolation routine (0: polynomial, 1: rational)
- Reduction factor for the TOUGH2 time step $\Delta t_{T2}$ if the BS stepper has reached the maximum number of time steps (default: 0.2)
- Error reduction factor $f_{ex}$ with $0 < f_{ex} < 1$ (default: 0.6)

The absolute tolerance decides on convergence if radionuclide quantities are small. If the absolute tolerance criterion is met for a specific radionuclide and location, transport and decay calculations are skipped.

Please note that adequate convergence criteria depend on the problem to be solved. Both, tolerance criteria and simulation controls of the RN module are likely to be further developed in the future.

## 16.4    Decay and adsorption of Nuclides

Radioactive decay is calculated for each time step $\Delta t_{T2}$ using an exponential decay law for each radionuclide:

$$N(t + \Delta t_{T2}) = N(t)e^{-\lambda \Delta t_{T2}} \tag{16.1}$$

$N$ is the amount of the radionuclide (mol), $\lambda$ the radioactive decay constant with

$$\lambda = \frac{\ln 2}{T_{1/2}}, \tag{16.2}$$

and $T_{1/2}$ the half-life of the radionuclide. The exponential decay function improves the implementation of TOUGH2, which uses a linear decay function with lower accuracy.

Since the radioactive decay is calculated for the entire time step, $\Delta t_{T2}$ should be kept smaller than the half-life of radionuclides in order to achieve sufficient accuracy. This may impose a performance problem which should be subject to future code development.

## 16.5 Anion exclusion

Usually, the pore space of argillaceous rocks is not fully accessible to anions, which are forced to the pore centres by the negative charge of mineral surfaces. This process is called anion exclusion and it can affect both, the advective and diffusive transport of radionuclides. In order to keep our model simple we assume that there is a sharp transition between the pore space accessible to anions and to that which is not. We will formulate our model for a single phase and a single anion to keep the description simple.

### Advective transport of anions

TOUGH2 calculates the advective mass flow $F_{adv}$ of a component (in kg/sec) by multiplying the mass flow of the fluid $F_{phase}$ by the mass fraction $X$ of the transported component:

$$F_{adv} = F_{phase}\ X \tag{16.3}$$

We use a similar approach for the advective transport of an anion in restricted pore space

$$F_{adv} = \hat{F}_{phase}\ \hat{X} . \tag{16.4}$$

$\hat{F}_{phase}$ denotes the flow of fluid in restricted pore space and $\hat{X}$ the anion's mass fraction in the fluid. If $\phi$ is porosity and $\phi_{ex}$ the porosity from which anions are excluded, $\hat{X}$ and $X$ are related by

$$\hat{X} = X \frac{\phi}{1 - \phi_{ex}} \tag{16.5}$$

because of the different fluid masses they refer to.

Obviously $\hat{X}$ is larger than $X$ but on the other hand, $\hat{F}_{\text{phase}}$ must be smaller than or equal to the total fluid flow $F_{\text{phase}}$.

To understand how $\hat{X}$ and $\hat{F}_{\text{phase}}$ interact we consider the physically impossible case that particle velocities are the same at every point of the pore space. Under these unrealistic conditions the restriction of anions to pore centers would have no influence on anion flow. Obviously, anion exclusion enhances advective anion transport only if the flow densities in the accessible pore space are higher than in the inaccessible pore space (which can be expected in reality). The effect of anion exclusion therefore depends on the heterogeneity of the flow field, which has to be expressed by a relation between $\hat{F}_{\text{phase}}$ and $F_{\text{phase}}$. We use

$$\hat{F}_{\text{phase}} = F_{\text{phase}} \left( 1 - R_{\text{flow}} \right) \tag{16.6}$$

for this purpose, where $R_{\text{flow}}$ is the fraction of the flow that is inaccessible to anions. The highest anion flow is achieved by $R_{\text{flow}} = 0$ meaning that the entire flow takes place in the accessible pore space. In the discrete version of this equation the element-specific variable $R_{\text{flow}}$ is weighted using the `WUP` parameter of input block PARAM.

In order to obtain $R_{\text{flow}}$, we revisit the above example of constant particle velocities. We have reasoned that anion exclusion should have no effect with constant particle velocities. This means that

$$\hat{F}_{\text{phase}} \, \hat{X} = F_{\text{phase}} \, X. \tag{16.7}$$

From this we can conclude that

$$R_{\text{flow}} = 1 - \frac{X}{\hat{X}} = \frac{1 - \phi_{\text{ex}}}{\phi}. \tag{16.8}$$

Consequently, the condition

$$0 \leq R_{\text{flow}} < \frac{1 - \phi_{\text{ex}}}{\phi} \tag{16.9}$$

should be met for natural porous media.

The case $R_{\text{flow}} = 0$ is particularly interesting for the derivation of benchmark calculations. Let us consider two systems, one without anion exclusion and porosity $\phi_1$ and another with anion exclusion and porosity $\phi_2$. If we set $R_{\text{flow}}$ to zero, the entire flow takes place in the anion-accessible pore space. Under these circumstances, anion transport should be the same in both systems if the anion-accessible porosity of the second system $\phi_2 - \phi_{\text{ex}}$ is equal to $\phi_1$. This also applies to the diffusive transport described below.

***Diffusive transport of anions***

TOUGH2's flow equation for the diffusive transport of a component between two grid elements is

$$F_{\text{diff}} = -A\,\phi\,\tau\,\rho\,d\,\nabla X \tag{16.10}$$

where $d$ is the molecular diffusion coefficient, $\rho$ the density of the phase, $\tau$ a geometry factor that can be determined in several ways, $\phi$ porosity, and $A$ the interface area between the two grid elements. Factor $A\phi$ is the interface area for the transport. The geometry factor $\tau$ captures effects of contorted flow paths and unsaturated conditions. Note that $\tau$ decreases with increasing tortuosity of flow paths.

For anion exclusion, $\phi$, $\tau$ and $X$ have to be substituted by corresponding parameters for the restricted flow path:

$$F_{\text{diff}} = -A\,\hat{\phi}\,\hat{\tau}\,\rho\,d\,\nabla\hat{X} \tag{16.11}$$

$\hat{X}$ has already been introduced and the new flow cross section $\hat{\phi}$ can be set equal to $\phi - \phi_{\text{ex}}$. We set the geometry factor to

$$\hat{\tau} = \tau(1 - R_{\text{tort}}) \tag{16.12}$$

using a reducing factor $1 - R_{\text{tort}}$, which should be smaller than one. Variables $\phi$ and $\tau$ are element specific. For element connections they are calculated in the same way as $d$ using a weighted harmonic mean.

In homogeneous material and if the geometry factor remains unchanged ($R_{\text{tort}} = 0$) the diffusive flow remains unchanged too, because $\hat{\phi}\,\nabla\hat{X} = \phi\,\nabla X$. Yet, under transient con-

ditions, anion exclusion still has an effect on diffusive transport owing to the fact that pore space is restricted and less flow is needed to propagate a diffusive front.

### *A note on inactive and active elements*

Radionuclides are introduced to active elements by prescribing radionuclide masses. From a physical point of view, these masses are only present in the pore space that is accessible to anions. Mean concentrations are obtained by dividing anion masses by the total pore volume. To obtain concentrations inside the accessible pore volume, radionuclide masses must be divided by the accessible pore volume.

Inactive elements require the prescription of mass concentrations in the accessible pore volume because of their unknown volume. Concentrations refer to radionuclide masses per *accessible* pore volume.

## 16.6      Extended mobilization models

### 16.6.1      New commands

TOUGH2-MP-GRS v. 0 and TOUGH2-GRS v. 2 introduce new models for radionuclide mobilization. These models are still under development.

Since TOUGH2-GRS v. 1, the standard method of placing radionuclides in the system is by using the command "`place`" (see chapter 16.7). This command places the mass of a certain radionuclide in a material. The command allows to specify a mobilization time. Until that time, radionuclides remain immobile and are subject to radioactive decay.

With TOUGH2-GRS v. 2 and TOUGH2-MP-GRS v. 0 additional mobilization models are introduced by the commands "`container`", "`bond`" and "`rn`". These commands are motivated as follows.

We assume that radionuclides are contained in a waste container by different bonds. For instance, the instant release fraction represents a certain bond type, but radionuclides can also be bound to a corroding waste matrix. Models for the mobilization of radionuclides from a specific bond will be called "bond models" in the following.

The release of radionuclides depends on the time of canisters failure too. We introduce "canister failure models" to describe the failure of a certain canister type. Canister failure models are not assigned to a single container but to a group of containers of same type.

Eventually, a "mobilization model" is a combination of a bond model and a canister failure model. Mobilization models take the general form

$$\dot{Q}(i,t) = n(t)\dot{Q}_{\text{pmob}}(i,t)\,, \tag{16.13}$$

$\dot{Q}(i,t):$      mobilization rate, i. e. mobilized mass per time for radionuclide $i$ at time $t$ in kg/s

$n(t) = N_{\text{fail}}(t)/N_{\text{tot}}:$ fraction of canisters that have failed

$\dot{Q}_{\text{pmob}}:$      rate of mobilization from the bond in kg/s

with $\dot{n}(t)$ being the canister failure model and $\dot{Q}_{\text{pmob}}(i,t)$ the bond model. The following commands are introduced for the definition of mobilization models (see also Tab. 16.2):

- The "container" command defines the location of a canister group and a corresponding container failure model.

- The "bond" command adds a bond type to the canister group that has been defined last (that is the last "canister" command).

- The "rn" command assigns radionuclides of a certain mass to the bond and canister group that have been defined last.

Radionuclides introduced in this way are not visible in the simulation output before they are mobilized.


## 16.6.2     Canister failure models

Canister failure models refer to a group of canisters (preferably of same type). The discrete failure of canisters is approximated by a continuous function, which is the canister failure model.

Canister failure models define a "trigger event" that starts the failure process. No canister fails before that event. The trigger event can be the start of the simulation (then there actually is no trigger) but also the accomplishment of a certain liquid saturation. For the time being there are two canister failure models: a constant failure rate and a normal distribution of failures.

**Constant failure rate**

A constant failure rate stands for a uniform distribution of canister life times. The canister failure rate is

$$\dot{n}(t) = \frac{\dot{N}_{\text{fail}}(t)}{N_{\text{tot}}} = \begin{cases} 0 & \text{for} & t < t_{\text{tw}} \\ 1/t_{\text{conf}} & \text{for} & t_{\text{tw}} \leq t < t_{\text{tw}} + t_{\text{conf}} \\ 0 & \text{for} & t > t_{\text{tw}} + t_{\text{conf}} \end{cases} \qquad (16.14)$$

$N_{\text{fail}}(t), \dot{N}_{\text{fail}}(t)$:  number of canisters that have failed, and failure rate

$N_{\text{tot}}$:  number of canisters

$t_{\text{tw}} := t_{\text{trig}} + t_{\text{wait}}$ with

$t_{\text{trig}} \geq 0$:  time of the trigger event

$t_{\text{wait}} \geq 0$:  time between trigger event and first failure

$t_{\text{conf}} \geq 0$:  here: time between first and last canister failure

The fraction of canisters that have failed is

$$n(t) = \frac{N_{\text{fail}}(t)}{N_{\text{tot}}} = \begin{cases} 0 & \text{for} & t < t_{\text{tw}} \\ \dfrac{t - t_{\text{tw}}}{t_{\text{conf}}} & \text{for} & t_{\text{tw}} \leq t < (t_{\text{tw}} + t_{\text{conf}}) \\ 1 & \text{for} & t > (t_{\text{tw}} + t_{\text{conf}}) \end{cases} \qquad (16.15)$$

The `"canister"` command requires the following numerical input parameters:

1. Selector for container failure model. Set to 1 for a constant rate.
2. Selector for the trigger event: Set to 0 for no trigger and to 1 for the excess of a certain liquid saturation.
3. Critical liquid saturation (for trigger event 1).
4. $t_{\text{conf}}$. Meaning here the time between the first and the last failure event. Set $t_{\text{conf}} = 0$ for instant failure of all canisters.
5. Waiting time $t_{\text{wait}}$ between trigger event and the first failure.

**Normal distribution of failures**

This model assumes that all canisters have a similar resistance against corrosion but canister failure frequency varies around a mean confinement time $t_{\text{conf}}$ according to a normal distribution. The canister failure rate is

$$\dot{n}(t) = \begin{cases} 0 & \text{for} \quad t < t_{\text{trig}} \\ \dfrac{1}{\sqrt{2\pi}\sigma}e^{-\frac{1}{2}\left(\frac{(t-t_{\text{trig}})-t_{\text{conf}}}{\sigma}\right)^2} & \text{for} \quad t \geq t_{\text{trig}} \end{cases} \tag{16.16}$$

$t_{\text{trig}} \geq 0:$    time of the trigger event

$t_{\text{conf}} \geq 0:$    here: mean canister life time

$\sigma:$        standard deviation of the canister life time

The fraction of canisters that have failed is

$$n(t) = \frac{1}{2}\left(1 + \text{erf}\left(\frac{(t - t_{\text{trig}}) - t_{\text{conf}}}{\sqrt{2\pi}}\right)\right) \tag{16.17}$$

The "canister" command requires the following numerical input parameters:

1. Selector for container failure model. Set to 2 for normal distribution.
2. Selector for the trigger event: Set to 0 for no trigger and to 1 for the excess of a certain liquid saturation.
3. Critical liquid saturation (for trigger event 1).
4. $t_{\text{conf}}$. Meaning here: mean canister life time
5. Standard deviation $\sigma$ of the canister life time

### 16.6.3 Bond models

Bond models take the following general form:

$$\dot{Q}_{\text{pmob}}(i,t;T,\ldots;T_{\text{acti}},\ldots) = \frac{m_{\text{ibin}}(i,t)}{m_{\text{bin}}(t)} \cdot (A_{\text{eff}} \cdot j_{\text{mobTr}}) \cdot e^{-T_{\text{acti}}\left(\frac{1}{T}-\frac{1}{T_{\text{ref}}}\right)} \tag{16.18}$$

$\dot{Q}_{\text{pmob}}(i,t,\ldots)$ : rate of mobilization from the bond in kg/s for radionuclide $i$ at time $t$. This function may depend on state variables like, for example, temperature or liquid saturation.

$T_{\text{ref}}$ : reference temperature in K.

$T_{\text{acti}}$ : activation temperature in K. Set to 0 for no temperature dependency.

$m_{\text{ibin}}/m_{\text{bin}}$ : mass fraction of radionuclide $i$ in the bond.

$A_{\text{eff}}$ : effective surface of waste canisters in m².

$j_{\text{mobTr}}$ : mobilization flow density $j_{\text{mobTr}}$ at reference temperature $T_{\text{ref}}$ in kg m$^{-2}$ s$^{-1}$

The "bond" command requires the following numerical input parameters:

1. Selector for the bond model. Set to 1.
2. Selector for the type of function $A_{\text{eff}}$. Set to 0 for a constant function.
3. First parameter of function $A_{\text{eff}}$. Value of $A_{\text{eff}}$ if a constant function has been selected.
4. Second parameter of function $A_{\text{eff}}$.
5. Third parameter of function $A_{\text{eff}}$.
6. Selector for type of function $j_{\text{mobTr}}$. Set to 0 for a constant function.
7. First parameter of function $j_{\text{mobTr}}$. Value of $j_{\text{mobTr}}$ if a constant function has been selected.
8. Second parameter of function $j_{\text{mobTr}}$.
9. Third parameter of function $j_{\text{mobTr}}$.
10. Activation temperature $T_{\text{acti}}$. Set to 0 for no temperature dependency.
11. Reference temperature $T_{\text{ref}}$.

### 16.6.4 Implementation

The Bulirsch-Stoer solver of the RN module used for time integration requires processes that change radionuclide masses continuously. Discontinuous mobilization process-

es like, for example, instant release therefore cannot be part of the time integration algorithm. Discontinuous transfer of radionuclides from their bonds into the flow system has to be carried out *before* the Bulirsch-Stoer algorithm. In principle, continuous mobilization processes can be implemented in the same way. To keep the implementation simple, we use this kind of radionuclide transfer for discontinuous as well as for continuous mobilization models. However, there are two disadvantages connected to this procedure:

- The release time of a discontinuous release must not match the simulation time steps. This causes an error in release times. In principle, this can be solved by adapting the automatic time stepping control to the release times.

- Continuous releases do not benefit from the higher time discretization of the Bulirsch-Stoer solver.

## 16.7 Input data

Tab. 16.1 show the syntax of control parameters and radionuclide definitions. The following command section of the input is described in Tab. 16.2.

**Tab. 16.1** Input format of data block RN

| Line | Co-lumn | Content | For-mat | Unit | Description | Variable |
|---|---|---|---|---|---|---|
| 1 | 1-10 | Relative tolerance | G10.4 | 1 | default: 1E-7 | rncntrl_relTol |
| | 11-20 | Absolute tolerance | G10.4 | kg | default: 1E-30 kg | rncntrl_absMtol |
| | 21-30 | Maximum steps of the Burlirsch-Stoer stepper | I10 | 1 | default: 1000 | rncntrl_maxstp |
| | 31-40 | extrapolation routine | I10 | 1 | 0: polynomial (default), 1: rational | rncntrl_extrRout |
| | 41-50 | Reduction factor for the TOUGH2 time step $\Delta t_{T2}$ if the BS stepper has reached the maximum number of time steps | G10.4 | 1 | default: 0.2 | rncntrl_dtFac |
| | 51-60 | Error reduction factor $f_{ex}$ with $0 < f_{ex} < 1$ | G10.4 | 1 | default: 0.6 | rncntrl_errFac |
| *Repeat the following lines for each radionuclide (RN) i* | | | | | | |
| 2+(i-1) | 1-10 | Radionuclide name | A10 | | Name of radionuclide (RN) | rn_NAME |
| | 11-21 | $T_{1/2}$ | G10.4 | s | Half-life of RN | rn_HALF |
| | 21-30 | RN Daughter name | A10 | | Name of daughter RN | rn_daughtername |
| | 31-40 | Molecular weight | G10.4 | kg/mol | Molecular weight of RN | rn_M |
| | 41-50 | Henry constant or inverse Henry constant | G10.4 | Pa or 1/Pa | Absolute value will be used. <0: use Henry constant >0: use inverse Henry constant | rn_H |
| | 51-60 | Solubility limit | G10.4 | kg/m³ | Solubility limit | rn_Ceq |
| | 61-70 | Diffusivity in gas | G10.4 | m²/s | Diffusion constant in gas phase | rn_Dg |
| | 71-80 | Diffusivity in liquid | G10.4 | m²/s | Diffusion constant in liquid phase | rn_Dl |
| *This section closes with a "--" line, which signals, that a command section follows (see next table)* | | | | | | |

**Tab. 16.2**   Commands of module RN

See chapters 16.6.2 and 16.6.3 for the parameters of canister failure and bond models.

| column 1 to 10 | column 11 to 20 | column 21 to 25 | column 26+(i-1)*10 to 40+(i-1)*10 |
|---|---|---|---|
| *command string (case insensitive)* | *string (A10)* | *string (A5)* | *list of numbers (G15.4)* |
| "place" | name of radionuclide (leave blank to select all radionuclides) | material name (leave blank to select all materials) | *active elements*: 1st: initial radionuclide mass in kg. *inactive elements*: 1st: initial radionuclide concentration in kg/m³. 2nd: time of release in sec. |
| "retard" | name of radionuclide (leave blank to select all radionuclides) | material name (leave blank to select all materials) | 1st: $K_d$ in m³/kg. |
| "exclusion" | name of radionuclide (leave blank to select all radionuclides) | material name (leave blank to select all materials) | 1st: excluded porosity fraction 2nd: flow reduction (between 0 and 1) 3rd: tortuosity reduction (between 0 and 1) |
| "container" | element name or material name | type of location ("E" for element, "M" for material) | 1st: container failure model (selector) next: parameters of container failure model |
| "bond" | *empty* | *empty* | 1st: selector for bond model (selector) next: parameters of bond model |
| "rn" | radionuclide name | *empty* | 1st: inserted mass in kg |

# 17 Output

TOUGH2-GRS and TOUGH2-MP-GRS generate two types of printouts:

- Total system printouts to the files ELE_MAIN and CON_MAIN for prescribed times.
- Time series printouts to the files FOFT, COFT, GOFT, and DOFT for prescribed elements, connections, sources, and domains (rocks), respectively.

The total system printout to the output channel STDOUT still exists but is not maintained anymore and will therefore not be mentioned in the following.

The process modules of GRS have increased the number of output parameters. To reduce file sizes, the module CNTRL allows to skip printouts (see chapter 4.3.2). Time series files can also be generated in binary format. Whether the time series output uses text or binary format is controlled by the CNTRL module.

## 17.1 Global printouts for elements (ELE_MAIN)

Global printouts to file ELE_MAIN are generated at user-defined times (specified in data blocks TIMES or PTIME) as well as on the first and last time step. The printout holds element-specific output data formatted in the same way as the time series files:
`time step number, time, [element index,[variables, …], …].`

**Tab. 17.1** Element-specific output parameters of TOUGH2-GRS

| No TOUGH2-GRS | No TOUGH2-MP-GRS | Module (0 printed if inactive) | Parameter | Description | Unit |
|---|---|---|---|---|---|
| 1 | 1 | | $P_{gas}$ | gas pressure | Pa |
| 2 | 2 | | $P_{liq} = P_{gas} + P_{cap}$ | liquid pressure | Pa |
| 3 | 3 | | $S_{liq}$ | gas saturation | 1 |
| 4 | 4 | | $S_{gas}$ | liquid saturation | 1 |
| 5 | 5 | | $X_{brine}$ | brine concentration | 1 |
| 6 | 6 | | $T$ | temperature | °C |
| 7 | 7 | | $-P_{cap}$ | capillary pressure ($P_{cap}$ is negative) | Pa |
| 8 | 8 | | $P_{pot} := P_{liq} - zg\rho_{liq}$ | pressure potential (only a potential if density is constant) | Pa |
| 9 | 9 | | $\rho_{gas}$ | density of the gas phase | kg/m³ |
| 10 | 10 | | $\rho_{liq}$ | density of the liquid phase | kg/m³ |
| 11 | 11 | | $\mu_{gas}$ | viscosity of the gas phase | Pa s |
| 12 | 12 | | $\mu_{liq}$ | viscosity of the liquid phase | Pa s |
| 13 | 13 | | $k$ | intrinsic permeability (ISO=1) multiplied by $V_{phys}/V_{tough}$ | m² |
| 14 | 14 | | $V_{tough}$ | initial element volume | m³ |
| 15 | 15 | COMP otherwise 1 | $V_{phys}/V_{tough}$ | fraction of the physical volume | 1 |
| 16 | 16 | COMP otherwise $\phi_{tough}$ | $\phi_{phys}$ | physical porosity, referring to $V_{phys}$ | 1 |
| 17 | 17 | | $\phi_{tough}$ | internal porosity of TOUGH, referring to $V_{tough}$ | 1 |
| 18 | 18 | FISS | $\phi_{fiss}$ | porosity of a fissure | 1 |
| 19 | 19 | FISS | $k_{fiss}$ | fissure permeability | Pa |
| 20 | 20 | FISS | $p_{thr}$ | pressure Threshold | Pa |
| 21 | 21 | COMP | $K$ | rate of convergence | 1/s |
| 22 | 22 | CORRO | $g$ | grade of canister corrosion (weighted average over sources) | 1 |
| 23 | 23 | CORRO | $Q$ | rate of gas generation | mol/s |
| 24 | 24 | CORRO | $m_{can}$ | canister water mass | kg |
| 25 | 25 | CORFL | $g$ | grade of seal corrosion | 1 |
| 26 | 26 | TFC | | TOUGH2-GRS/TFC: SIGMAJVEC TOUGH2-MP-GRS: outflow gas (x-component) | Pa kg/m²/s |
| 27 | 27 | TFC | | TOUGH2-GRS/TFC: SIGMEDVEC TOUGH2-MP-GRS: outflow gas (y-component) | Pa kg/m²/s |
| 28 | 28 | TFC | | TOUGH2-GRS/TFC: SIGMINVEC TOUGH2-MP-GRS: outflow gas (z-component) | Pa kg/m²/s |
| 29 | 29 | TFC | | TOUGH2-GRS/TFC: ACTVOLVEC TOUGH2-MP-GRS: outflow liq. (x-component) | Pa kg/m²/s |
| 30 | 30 | TFC | | TOUGH2-GRS/TFC: MINEFFSTRESS TOUGH2-MP-GRS: outflow liq. (y-component) | Pa kg/m²/s |

| No TOUGH2-GRS | No TOUGH2-MP-GRS | Module (0 printed if inactive) | Parameter | Description | Unit |
|---|---|---|---|---|---|
| 31 | 31 | TFC | | TOUGH2-GRS/TFC: MEANEFFSTRESS<br>TOUGH2-MP-GRS: outflow liq. (z-component) | Pa<br>kg/m²/s |
| 32 | 32 | TFC | | TOUGH2-GRS/TFC: PERFAC<br>TOUGH2-MP-GRS: 0 | Pa |
| 33 | 33 | EOS7R | $X_{\text{RN1}}^{\text{gas}}$ | mass fraction of RN 1 in the gas phase | 1 |
| 34 | 34 | EOS7R | $X_{\text{RN1}}^{\text{liq}}$ | mass fraction of RN 1 in the liquid phase | 1 |
| 35 | 35 | EOS7R | $X_{\text{RN2}}^{\text{gas}}$ | mass fraction of RN 2 in the gas phase | 1 |
| 36 | 36 | EOS7R | $X_{\text{RN2}}^{\text{liq}}$ | mass fraction of RN 2 in the liquid phase | 1 |
| 37 | 37 | | | number of maximal residua since last print out | 1 |
| 38 | 38 | | | Condition of aggregation<br>(1: gas phase only; 2: two-phase; 3: liquid phase only) | 1 |
| 39 | 39 | | $\dfrac{dP_{\text{cap}}}{dS_{\text{liq}}}$ | dPcap/dSliq<br>(for elements with two-phase condition only; always positive) | Pa |
| *The following lines are repeated for each radionuclide of the RN module* | | | | | |
| 40+7*(i-1) | 40+6*(i-1) | RN | $m_{\text{RN i}}^{\text{tot}}$ | mass of RN i (0 for inactive elements) | kg |
| 41+7*(i-1) | 41+6*(i-1) | RN | $X_{\text{RN i}}^{\text{gas}}$ | mobile concentration of. RN i in the gas phase | 1 |
| 42+7*(i-1) | 42+6*(i-1) | RN | $X_{\text{RN i}}^{\text{liq}}$ | mobile concentration of. RN i in the liquid phase | 1 |
| 43+7*(i-1) | 43+6*(i-1) | RN | $m_{\text{RN i}}^{\text{gas}}$ | mobile mass of RN i in the gas phase(0 for inactive elements) | kg |
| 44+7*(i-1) | 44+6*(i-1) | RN | $m_{\text{RN i}}^{\text{liq}}$ | mobile mass of RN i in the liquid phase(0 for inactive elements) | kg |
| 45+7*(i-1) | 45+6*(i-1) | RN | $m_{\text{RN i}}^{\text{ads}}$ | adsorped mass of RN I (0 for inactive elements) | kg |
| 46+7*(i-1) | | RN | | \|OutflowAdv\|-\|OutflowDiff\| | kg/s |

## 17.2    Global printouts for connections (CON_MAIN)

Global printouts are generated at user-defined times (which are specified in data blocks TIMES or PTIME) as well as on the first and last time step. The printout to file CON_MAIN contains connection-specific output using the same format as the time series files `time step number, time, [element index,[variables, …], …]`. If `MOPR(24)=0` (default) the diffusive flux in gas is 0 and the outputted diffusive flux in liquid holds the full multiphase diffusive flux. For `MOPR(24)=1` the diffusive flow is calculated for each phase separately. The fluxes are positive if flow is directed from the second to the first element of a connection.

**Tab. 17.2** Connection-specific parameters in TOUGH2-GRS

| No | Module (0 printed if inactive) | Parameter | Description | Unit |
|---|---|---|---|---|
| 1 | | $Q^{\text{heat}}$ | heat flow | J/s |
| 2 | | $E_s$ | specific energy | J/kg |
| 3 | | $Q^{\text{tot}}$ | Total mass flow | kg/s |
| 4 | | $Q^{\text{gas}}$ | mass flow in the gas phase | kg/s |
| 5 | | $Q^{\text{liq}}$ | mass flow in the liquid phase | kg/s |
| 6 | | $Q^{\text{liq}}_{\text{brine}}$ | Total mass flow | kg/s |
| 7 | | $v_{gas}$ | pore velocity in the gas phase | m/s |
| 8 | | $v_{liq}$ | pore velocity in the liquid phase | m/s |
| 9 | EOS7R | $Q^{\text{adv,gas}}_{\text{RN1}}$ | advective flow of RN1 (gas phase) | kg/s |
| 10 | EOS7R | $Q^{\text{adv,gas}}_{\text{RN2}}$ | advective flow of RN2 (gas phase) | kg/s |
| 11 | EOS7R | $Q^{\text{adv,liq}}_{\text{RN1}}$ | advective flow of RN1 (liquid phase) | kg/s |
| 12 | EOS7R | $Q^{\text{adv,liq}}_{\text{RN2}}$ | advective flow of RN2 (liquid phase) | kg/s |
| 13 | | $Q^{\text{dif,gas}}_{H_2O}$ | diffusive flow of water (gas phase) | kg/s |
| 14 | | $Q^{\text{dif,gas}}_{\text{brine}}$ | diffusive flow of brine (gas phase) | kg/s |
| 15 | | $Q^{\text{dif,gas}}_{\text{air}}$ | diffusive flow of air (gas phase) | kg/s |
| 16 | EOS7R | $Q^{\text{dif,gas}}_{\text{RN1}}$ | diffusive flow of RN1 (gas phase) | kg/s |
| 17 | EOS7R | $Q^{\text{dif,gas}}_{\text{RN2}}$ | diffusive flow of RN2 (gas phase) | kg/s |
| 18 | | $Q^{\text{dif,liq}}_{H_2O}$ | diffusive flow of water (liquid phase) | kg/s |
| 19 | | $Q^{\text{dif,liq}}_{\text{brine}}$ | diffusive flow of brine (liquid phase) | kg/s |
| 20 | | $Q^{\text{dif,liq}}_{\text{air}}$ | diffusive flow of air (liquid phase) | kg/s |
| 21 | EOS7R | $Q^{\text{dif,liq}}_{\text{RN1}}$ | diffusive flow of RN1 (liquid phase) | kg/s |
| 22 | EOS7R | $Q^{\text{dif,liq}}_{\text{RN2}}$ | diffusive flow of RN2 (liquid phase) | kg/s |
| *The following lines are repeated for each radionuclide of the RN module* | | | | |
| 23+5*(i-1) | RN | $Q^{\text{tot}}_{\text{RN i}}$ | mass flow of RN i | kg/s |
| 24+5*(i-1) | RN | $Q^{\text{adv,gas}}_{\text{RN i}}$ | advective flow of RN i (gas phase) | kg/s |
| 25+5*(i-1) | RN | $Q^{\text{dif,gas}}_{\text{RN i}}$ | diffusive flow of RN i (gas phase) | kg/s |
| 26+5*(i-1) | RN | $Q^{\text{adv,liq}}_{\text{RN i}}$ | advective flow of RN i (liquid phase) | kg/s |
| 27+5*(i-1) | RN | $Q^{\text{dif,liq}}_{\text{RN i}}$ | diffusive flow of RN i (liquid phase) | kg/s |

## 17.3        Time series for elements (FOFT)

These printouts are generated for user-defined elements specified in data block FOFT. The frequency of printouts can be customized by data block CNTRL.

**Tab. 17.3**   Element-specific parameters in `FOFT`

| No | Module (0 printed if inactive) | Parameter | Description | Unit |
|----|--------------------------------|-----------|-------------|------|
| 1 | | $P_{\text{gas}}$ | gas pressure | Pa |
| 2 | | $P_{\text{liq}} = P_{\text{gas}} + P_{\text{cap}}$ | liquid pressure | Pa |
| 3 | | $S_{\text{gas}}$ | gas saturation | 1 |
| 4 | | $S_{\text{liq}}$ | liquid saturation | 1 |
| 5 | | $X_{\text{brine}}$ | brine concentration | 1 |
| 6 | | $T$ | temperature | °C |
| 7 | | $-P_{\text{cap}}$ | capillary pressure (in TOUGH2 $P_{\text{cap}}$ is negative thus the output is positive) | Pa |
| 8 | | $P_{\text{pot}} = P_{\text{liq}} - zg\rho_{\text{liq}}$ | pressure potential (only a potential if density is constant) | Pa |
| 9 | | $\rho_{\text{gas}}$ | density of the gas phase | kg/m³ |
| 10 | | $\rho_{\text{liq}}$ | density of the liquid phase | kg/m³ |
| 11 | | $\mu_{\text{gas}}$ | viscosity of the gas phase | Pa s |
| 12 | | $\mu_{\text{liq}}$ | viscosity of the liquid phase | Pa s |
| 13 | | $k$ | intrinsic permeability (for ISO=1) multiplied by the area reduction factor $V_{\text{phys}}/V_{\text{tough}}$ | m² |
| 14 | | $V_{\text{tough}}$ | initial element volume | m³ |
| 15 | COMP otherwise 1 | $V_{\text{phys}}/V_{\text{tough}}$ | fraction of the physical element volume $V_{\text{phys}}/V_{\text{tough}}$ | 1 |
| 16 | COMP otherwise $\phi_{\text{tough}}$ | $\phi_{\text{phys}}$ | physical porosity, referring to $V_{\text{phys}}$ | 1 |
| 17 | | $\phi_{\text{tough}}$ | internal porosity of TOUGH, referring to $V_{\text{tough}}$ | 1 |
| 18 | FISS | $\phi_{\text{fiss}}$ | fissure porosity | 1 |
| 19 | FISS | $k_{\text{fiss}}$ | fissure permeability | m² |
| 20 | FISS | $p_{\text{thr}}$ | pressure threshold | Pa |
| 21 | COMP | $K$ | rate of convergence | 1/s |
| 22 | CORRO | $g$ | grade of corrosion (weighted average over sources) | 1 |
| 23 | CORRO | $Q$ | gas generation rate | mol/s |
| 24 | CORRO | $m_{\text{can}}$ | canister water mass | kg |
| 25 | CORFL | $g$ | grade of corrosion | 1 |
| 26 | EOS7R | $X_{\text{RN1}}^{\text{gas}}$ | mass fraction of RN 1 in the gas phase | 1 |
| 27 | EOS7R | $X_{\text{RN1}}^{\text{liq}}$ | mass fraction of RN 1 in the liquid phase | 1 |
| 28 | EOS7R | $X_{\text{RN2}}^{\text{gas}}$ | mass fraction of RN 2 in the gas phase | 1 |
| 29 | EOS7R | $X_{\text{RN2}}^{\text{liq}}$ | mass fraction of RN 2 in the liquid phase | 1 |

| No | Module (0 printed if inactive) | Parameter | Description | Unit |
|---|---|---|---|---|
| 30 | | $m_{H_2O}^{gas}$ | mass of water in the gas phase | kg |
| 31 | | $m_{H_2O}^{liq}$ | mass of water in the liquid phase | kg |
| 32 | | $m_{brine}^{gas}$ | mass of brine in the gas phase | kg |
| 33 | | $m_{brine}^{liq}$ | mass of brine in the liquid phase | kg |
| 34 | | $m_{air}^{gas}$ | mass of air in the gas phase | kg |
| 35 | | $m_{air}^{liq}$ | mass of air in the liquid phase | kg |
| 36 | EOS7R | $m_{RN1}^{gas}$ | mass of RN1 in the gas phase | kg |
| 37 | EOS7R | $m_{RN1}^{liq}$ | mass of RN1 in the liquid phase | kg |
| 38 | EOS7R | $m_{RN2}^{gas}$ | mass of RN2 in the gas phase | kg |
| 39 | EOS7R | $m_{RN2}^{liq}$ | mass of RN2 in the liquid phase | kg |
| 40 | EOS7R | $m_{RN1}^{ads}$ | adsorbed mass of RN1 | kg |
| 41 | EOS7R | $m_{RN2}^{ads}$ | adsorbed mass of RN2 | kg |
| *The following lines are repeated for each radionuclide of the RN module* | | | | |
| 42+6*(i-1) | RN | $m_{RN\ i}^{tot}$ | mass of RN i (0 for inactive elements) | kg |
| 43+6*(i-1) | RN | $X_{RN\ i}^{gas}$ | concentration of mobile RN i in the gas phase | 1 |
| 44+6*(i-1) | RN | $X_{RN\ i}^{liq}$ | concentration of mobile RN i in the liquid phase | 1 |
| 45+6*(i-1) | RN | $m_{RN\ i}^{gas}$ | mass of mobile RN i in the gas phase (0 for inactive elements) | kg |
| 46+6*(i-1) | RN | $m_{RN\ i}^{liq}$ | mass of mobile RN i in the liquid phase (0 for inactive elements) | kg |
| 47+6*(i-1) | RN | $m_{RN\ i}^{ads}$ | adsorbed mass of RN I (0 for inactive elements) | kg |

## 17.4    Time series for connections (COFT)

These printouts are generated for user-defined connections specified in data block COFT. The frequency of printouts can be customized by data block CNTRL. See chapter 0 for remarks on the effect of input parameter `MOP(24)` of data block PARAM.

**Tab. 17.4**    Connection-specific parameters in `COFT`

| No (KDATA ≠ 4) | No (KDATA= 4) | Module (0 printed if inactive) | Parameter | Description | Unit |
|---|---|---|---|---|---|
| 1 | 1 | | $Q^{\text{gas}}$ | mass flow in the gas phase | kg/s |
| 2 | 2 | | $Q^{\text{liq}}$ | mass flow in the liquid phase | kg/s |
| 3 | 3 | | $Q^{\text{heat}}$ | heat flow | J/s |
| | 4 | EOS7R | $Q_{\text{RN1}}^{\text{adv,gas}}$ | advective flow of RN1 (gas phase) | kg/s |
| | 5 | EOS7R | $Q_{\text{RN1}}^{\text{adv,liq}}$ | advective flow of RN1 (liquid phase) | kg/s |
| | 6 | EOS7R | $Q_{\text{RN1}}^{\text{adv,tot}}$ | advective flow of RN1 (both phases) | kg/s |
| | 7 | EOS7R | $Q_{\text{RN2}}^{\text{adv,gas}}$ | advective flow of RN2 (gas phase) | kg/s |
| | 8 | EOS7R | $Q_{\text{RN2}}^{\text{adv,liq}}$ | advective flow of RN2 (liquid phase) | kg/s |
| | 9 | EOS7R | $Q_{\text{RN2}}^{\text{adv,tot}}$ | advective flow of RN2 (both phases) | kg/s |
| | 10 | EOS7R | $Q_{\text{RN1}}^{\text{dif,gas}}$ | diffusive flow of RN1 (gas phase) | kg/s |
| | 11 | EOS7R | $Q_{\text{RN2}}^{\text{dif,gas}}$ | diffusive flow of RN2 (gas phase) | kg/s |
| | 12 | EOS7R | $Q_{\text{RN1}}^{\text{dif,gas}}$ | diffusive flow of RN1 (gas phase) | kg/s |
| | 13 | EOS7R | $Q_{\text{RN2}}^{\text{dif,gas}}$ | diffusive flow of RN2 (gas phase) | kg/s |
| 4 | 14 | EOS7R | $Q_{\text{RN1}}^{\text{tot}}$ | total mass flow RN1 (advection and diffusion) | kg/s |
| 5 | 15 | EOS7R | $Q_{\text{RN2}}^{\text{tot}}$ | total mass flow RN2 (advection and diffusion) | kg/s |
| *The following lines are repeated for each radionuclide if the RN module is active* | | | | | |
| 5+i | 16+5*(i-1) | RN | $Q_{\text{RN }i}^{\text{tot}}$ | total mass flow RN i | kg/s |
| | 17+5*(i-1) | RN | $Q_{\text{RN }i}^{\text{adv,gas}}$ | advective flow of RN i (gas phase) | kg/s |
| | 18+5*(i-1) | RN | $Q_{\text{RN }i}^{\text{adv,liq}}$ | advective flow of RN i (liquid phase) | kg/s |
| | 19+5*(i-1) | RN | $Q_{\text{RN }i}^{\text{dif,gas}}$ | diffusive flow of RN i (gas phase) | kg/s |
| | 20+5*(i-1) | RN | $Q_{\text{RN }i}^{\text{dif,liq}}$ | diffusive flow of RN i (liquid phase) | kg/s |

## 17.5    Time series for sinks and sources (GOFT)

These printouts are generated for user-defined sinks and sources specified in data block GOFT.

**Tab. 17.5**    Sink- and source-specific parameters in GOFT

| No | Parameter | Description | Unit |
|----|-----------|-------------|------|
| 1 | $N$ | generated component | 1 |
| 2 | $\dot{m}$ | mass generation rate | kg/s |
| 3 | $\dot{Q}$ | heat generation rate | J/s |
| 4 | $\int_{o}^{t} \dot{m}\,dt$ | generated mass at time $t$ | kg |
| 5 | $\int_{o}^{t} \dot{Q}\,dt$ | generated heat at time $t$ | J |

## 17.6    Time series for domains (DOFT)

These printouts are generated for user-defined domains (rocks) in data block DOFT. The first domain of the output is the entire domain of active elements, which is not specified in the input data block DOFT. For this reason the first domain specified in data block DOFT corresponds to the second domain in the output.

**Tab. 17.6**    Material-specific parameters in `DOFT`

| No. for KDATA ≠ 4 | No. for KDATA = 4 | Module (0 if inactive) | Parameter | Description | Unit |
|---|---|---|---|---|---|
| 1 | 1 | CORRO | $N^{\text{gas}}$ | amount of gas produced by corrosion | mol |
| 2 | 2 | CORRO | $m_{\text{can}}$ | canister water mass | kg |
| 3 | 3 | PRLIM | $V_{\text{esc}}$ | gas lost due to clippling | m3 |
| 4 | 4 | | $P_{\text{gas,max}}$ | maximal gas pressure | Pa |
| 5 | 5 | | $N_{\text{gas,max}}$ | material index for the location of maximal gas pressure | |
| | 6 | EOS7R | $m_{\text{RN1}}/V_i$ | mass of RN1 per volume of material i | kg/m3 |
| | 7 | EOS7R | $m_{\text{RN2}}/V_i$ | mass of RN2 per volume of material i | kg/m3 |
| | 8 | EOS7R | $R_{\text{max,RN1}}$ | maximal residuum of RN1 | |
| | 9 | EOS7R | $R_{\text{max,RN2}}$ | maximal residuum of RN2 | |
| | 10 | EOS7R | $\rho_{\text{max,RN1}}$ | density of RN1 for material with maximal residuum | kg/m3 |
| | 11 | EOS7R | $\rho_{\text{max,RN2}}$ | density of RN2 for material with maximal residuum | kg/m3 |
| | 12 – 15 | | | *obsolete* | |
| 6 | 16 | | $m_{H_2O}^{\text{gas}}$ | mass of water in the gas phase | kg |
| 7 | 17 | | $m_{H_2O}^{\text{liq}}$ | mass of water in the liquid phase | kg |
| 8 | 18 | | $m_{\text{brine}}^{\text{gas}}$ | mass of brine in the gas phase | kg |
| 9 | 19 | | $m_{\text{brine}}^{\text{liq}}$ | mass of brine in the liquid phase | kg |
| 10 | 20 | | $m_{\text{air}}^{\text{gas}}$ | mass of air in the gas phase | kg |
| 11 | 21 | | $m_{\text{air}}^{\text{liq}}$ | mass of air in the liquid phase | kg |
| 12 | 22 | EOS7R | $m_{\text{RN1}}^{\text{gas}}$ | mass of RN1 in the gas phase | kg |
| 13 | 23 | EOS7R | $m_{RN1}^{\text{liq}}$ | mass of RN1 in the liquid phase | kg |
| 14 | 24 | EOS7R | $m_{\text{RN2}}^{\text{gas}}$ | mass of RN2 in the gas phase | kg |
| 15 | 25 | EOS7R | $m_{RN2}^{\text{liq}}$ | mass of RN2 in the liquid phase | kg |
| *The following lines are repeated for each radionuclides of the RN module* | | | | | |
| 15+i | 26+3*(i-1) | RN | $m_{\text{RN}\,i}^{\text{tot}}$ | mass of RN i (0 for inactive elements) | kg |
| | 27+3*(i-1) | RN | $m_{\text{RN}\,i}^{\text{gas}}$ | mobile mass of RN i in the gas phase | kg |
| | 28+3*(i-1) | RN | $m_{\text{RN}\,i}^{\text{liq}}$ | mobile mass of RN i in the liquid phase | kg |

# References

GRS-A reports have been sponsored by the Federal Ministry for the Environment, Nature Conservation and Nuclear Safety (BMU). Quoting from these reports, reproducing them in whole or in parts or making them accessible to third parties requires the consent of BMU.

/BFS 09/ Bundesamt für Strahlenschutz (BfS): Sicherheitsanalyse für das verfüllte und verschlossene Endlager mit dem Programmpaket EMOS. P278, BfS-KZL: 9M/23210051/EG/RB/0056/00, 27 March 2009.

/FIS 01/ Fischer-Appelt, K., Fischer, H., Javeri, V., Martens, K.-H., Röhlig, K.-J., Eugen, S.: Implementierung von nichtlinearen Sorptionsansätzen in die Transportrechenprogramme MARNIE, NAMMU und TOUGH2 und deren Überprüfung. Gesellschaft für Anlagen- und Reaktorsicherheit (GRS) mbH, GRS-A-2897, 1 January 2001.

/GEN 80/ Genuchten, M. T. van: A Closed-form Equation for Predicting the Hydraulic Conductivity of Unsaturated Soils. Soil Science Society of America Journal, Vol. 44, No. 5, pp. 892–898, DOI 10.2136/sssaj1980.03615995004400050002x, 1980.

/GRA 14/ Grant, S. A., Bachmann, J.: Effect of Temperature on Capillary Pressure. Ed.: www.researchgate.net, available from , as at 2014.

/HOT 17/ Hotzel, S., Navarro, M., Seher, H.: QS-Handbuch für den Programmcode TOUGH2-GRS. GRS-401, ISBN 978-3-944161-82-2, Gesellschaft für Anlagen- und Reaktorsicherheit (GRS) gGmbH: Köln, 2017.

/JAV 95/ Javeri, V.: Orientierende Analysen zum Nuklidtransport durch Naturkonvektion; Gesteinskonvergenz und Dispersion in porösen Medien mit dem Rechenprogramm TOUGH2. Gesellschaft für Anlagen- und Reaktorsicherheit (GRS) mbH, GRS-A-2240: Köln, 1995.

/JAV 01/    Javeri, V.: Dreidimensionale Analysen zum Nuklidtransport bei salzanteil-
            abhängiger Adsorption in einem porösen Medium mit dem Rechenpro-
            gramm TOUGH2. Gesellschaft für Anlagen- und Reaktorsicherheit (GRS)
            mbH, GRS-A-2864: Köln, 2001.

/JAV 02/    Javeri, V.: Analysen zum Nuklidtransport bei variabler Salinität und nichtli-
            nearer Adsorption in der stark heterogenen Geosphäre der Gorlebener
            Rinne. Gesellschaft für Anlagen- und Reaktorsicherheit (GRS) mbH, GRS-
            A-3038: Köln, 2002.

/JUN 17/    Jung, Y., Pau, G. S. H., Finsterle, S., Pollyea, R. M.: TOUGH3, A new effi-
            cient version of the TOUGH suite of multiphase flow and transport simula-
            tors. Computers & Geosciences, Vol. 108, pp. 2–7, DOI
            10.1016/j.cageo.2016.09.009, 2017.

/KOC 12/    Kock, I., Eickemeier, R., Frieling, G., Heusermann, S., Knauth, M., Minkley,
            W., Navarro, M., Nipp, H.-K., Vogel, P.: Integritätsanalyse der geologischen
            Barriere, Bericht zum Arbeitspaket 9.1, Vorläufige Sicherheitsanalyse für
            den Standort Gorleben. Gesellschaft für Anlagen- und Reaktorsicherheit
            (GRS) mbH, GRS-286, 301 p., ISBN 978-3-939355-62-5: Köln, 2012.

/KOC 16/    Kock, I., Frieling, G., Navarro, M.: Fluidströmung und Radionuklidtransport
            in komplexen Endlagerbergwerken, Synthesebericht Teil 1/2, Zweiphasen-
            fluss in einem salinaren Endlager am Beispiel des ERAM. GRS-399, ISBN
            978-3-944161-80-8, Gesellschaft für Anlagen- und Reaktorsicherheit (GRS)
            gGmbH: Köln, 2016.

/KRÖ 09/    Kröhn, K. P., Stührenberg, D., Herklotz, M., Heemann, U., Lerch, C., Xie,
            M.: Restporosität und -permeabilität von kompaktierendem Salzgrus-
            Versatz in einem HAW-Endlager - Phase 1. Gesellschaft für Anlagen- und
            Reaktorsicherheit (GRS) mbH, GRS-254, 266 p., ISBN 978-3-939355-29-8,
            2009.

/LAR 13/    Larue, P.-J., Baltes, B., Fischer, H., Frieling, G., Kock, I., Navarro, M., Seher, H.: Radiologische Konsequenzenanalyse, Bericht zum Arbeitspaket
10, Vorläufige Sicherheitsanalyse für den Standort Gorleben. GRS-289,
267 p., ISBN 978-3-939355-65-6, Gesellschaft für Anlagen- und Reaktorsicherheit (GRS) mbH: Köln, 2013.

/LBNL 16/   Lawrence Berkeley National Laboratory (LBNL): TOUGH2 V2.0: Bugs and
Fixes. available from http://esd1.lbl.gov/research/projects/tough/software/
BugFixes.html, retrieved on 9 February 2016.

/LEV 41/    Leverett, M. C.: Capillary behaviour in porous solids. Transactions of the
AIME, Vol. 142, pp. 159–172, 1941.

/NAV 08/    Navarro, M., Baltes, B., Beuth, T., Bracke, G., Fischer, H., Fischer-Appelt,
K., Hotzel, S., Javeri, V., Kindt, A., Lambers, L., Larue, P.-J., McStocker,
B., Oppermann, U., Schrödl, E.: Verfolgung und Bewertung der Fortentwicklung des Standes von Wissenschaft und Technik beim Nachweis der
Langzeitsicherheit von Endlagern, Abschlussbericht zum Vorhaben SR
2548. Gesellschaft für Anlagen- und Reaktorsicherheit (GRS) mbH, GRS-
A-3418: Köln, 2008.

/NAV 09/    Navarro, M.: Simulating the migration of repository gases through argillaceous rock by implementing the mechanism of pathway dilation into the
code TOUGH2 (TOUGH2-PD), PAMINA project, public milestone 3.2.14.
Gesellschaft für Anlagen- und Reaktorsicherheit (GRS) mbH, Community
Research, 59 p., European Commission (EC): Brüssel, September 2009.

/NAV 13a/   Navarro, M.: Modelling Gas and Water Flow Through Dilating Pathways in
Opalinus Clay, The HG-C and HG-D Experiments, A study within the Euratom 7th Framework Programme Project FORGE. Gesellschaft für Anlagen- und Reaktorsicherheit (GRS) mbH, GRS-306, ISBN 978-3-939355-85-
4: Cologne, 2013.

/NAV 13b/   Navarro, M.: Handbuch zum Code TOUGH2-GRS.00a, Erweiterungen des
Codes TOUGH2 zur Simulation von Strömungs- und Transportprozessen in
Endlagern. Gesellschaft für Anlagen- und Reaktorsicherheit (GRS) mbH,
GRS-310, 75 p., ISBN 978-3-939355-89-2: Köln, 2013.

/NAV 13c/ Navarro, M.: Die vereinfachte Berechnung der Konvergenzrate salzgrusver-
füllter Hohlräume im Steinsalz. GRS-307, 47 p., ISBN 978-3-939355-86-1,
Gesellschaft für Anlagen- und Reaktorsicherheit (GRS) mbH: Köln, 2013.

/NAV 15/ Navarro, M.: Speeding up the iterative solvers of the T2SOLV solver pack-
age, A presentation at the TOUGH-Symposium 2015 at the Lawrence Ber-
eley National Laboratories. as at 2015, available from , retrieved on
04.05.16.

/NAV 16a/ Navarro, M., Eckel, J.: TOUGH2-GRS, Version 1, User Manual. GRS-403,
87 p., ISBN 978-3-944161-84-6, Gesellschaft für Anlagen- und Reaktorsi-
cherheit (GRS) gGmbH: Köln, July 2016.

/NAV 16b/ Navarro, M., Fischer, H., Seher, H., Weyand, T.: Ansätze zur Simulation
der Zweiphasenströmung in salinaren Endlagern mit dem Code TOUGH2-
GRS, Bericht im Vorhaben ZIESEL, Zweiphasenfluss in einem salinaren
Endlager am Beispiel des ERAM. GRS-398, 139 p., ISBN 978-3-944161-
79-2, Gesellschaft für Anlagen- und Reaktorsicherheit (GRS) gGmbH: Köln,
October 2016.

/NAV 18/ Martin Navarro, Jens Eckel, Heidemarie Fischer, Stephan Hotzel, Ingo
Kock: Test Handbook, TOUGH2-GRS Version 2, TOUGH2-MP-GRS Ver-
sion 0. GRS-402, ISBN 978-3-944161-83-9, Gesellschaft für Anlagen- und
Reaktorsicherheit (GRS) gGmbH: Köln, 2018.

/NOS 05/ Noseck, U., Brewitz, W., Becker, D.-A., Buhmann, D., Fahrenholz, C., Fein,
E., Hirsekorn, R.-P., Keesmann, S., Kröhn, K.-P., Müller-Lyda, I., Rübel, A.,
Schneider, A., Storck, R.: Wissenschaftliche Grundlagen zum Nachweis
der Langzeitsicherheit von Endlagern. Gesellschaft für Anlagen- und Reak-
torsicherheit (GRS) mbH, GRS-204, 205 p., ISBN 3-931995-71-2: Köln,
Garching b. München, Berlin, Braunschweig, 2005.

/PRU 99/ Pruess, K., Oldenburg, C., Moridis, G.: TOUGH2 User's Guide, Version 2.0.
Lawrence Berkeley National Laboratory (LBNL), LBNL-43134, 198 p.:
Berkeley, California, USA, 1 November 1999, revised September 2012.

/SEH 16/    Seher, H., Navarro, M.: SITA, Version 0, A simulation and code testing assistant for TOUGH2 and MARNIE. GRS-400, 78 p., ISBN 978-3-944161-81-5, Gesellschaft für Anlagen- und Reaktorsicherheit (GRS) gGmbH: Köln, June 2016.

/STE 85/    Stelte, N.: Analytische Approximation der Konvergenzrate salzgrusversetzter und unter hydraulischem Druck stehender Hohlräume im Salzgestein. In: Projekt Sicherheitsstudien Entsorgung (PSE) (Ed.): Einzeluntersuchungen zur Radionuklidfreisetzung aus einem Modellsalzstock, Fachband 15. pp. 108–141, TU Berlin: Berlin, 1985.

/STO 80/    Stoer, J., Bulirsch, R.: Introduction to Numerical Analysis. 609 p., ISBN 978-1-4757-5594-7, Springer New York: New York, NY, 1980.

/ZHA 08/    Zhang, K., Wu, Y.-S., Pruess, K.: User's Guide for TOUGH2-MP - A Massively Parallel Version of the TOUGH2 Code. Lawrence Berkeley National Laboratory (LBNL), LBNL-315E: Berkeley, California, USA, 1 May 2008.

# List of Figures

## List of Tables

# Acknowledgements